

# Schrödinger's Hat: Electromagnetic, acoustic and quantum amplifiers via transformation optics

Allan Greenleaf<sup>1,\*</sup>, Yaroslav Kurylev<sup>2</sup>, Matti Lassas<sup>3</sup> and Gunther Uhlmann<sup>4</sup>

<sup>1</sup>*Dept. of Mathematics, University of Rochester, Rochester, NY 14627*

<sup>2</sup>*Dept. of Mathematical Sciences, University College London, London, WC1E 6BT, UK*

<sup>3</sup>*Dept. of Mathematics, University of Helsinki, FIN-00014, Finland,*

<sup>4</sup>*Dept. of Mathematics, University of Washington, Seattle, WA 98195 and*

*Dept. of Mathematics, University of California, Irvine, CA 92697*

*\*Authors are listed in alphabetical order*

(Version of July 22, 2011)

## Abstract

The advent of transformation optics and metamaterials has made possible devices producing extreme effects on wave propagation. Here we give theoretical designs for devices, *Schrödinger hats*, acting as invisible concentrators of waves. These exist for any wave phenomenon modeled by either the Helmholtz or Schrödinger equations, e.g., polarized waves in EM, pressure waves in acoustics and matter waves in QM, and occupy one part of a parameter space continuum of wave-manipulating structures which also contains standard transformation optics based cloaks, resonant cloaks and cloaked sensors. For EM and acoustic Schrödinger hats, the resulting centralized wave is a localized excitation. In QM, the result is a new charged quasiparticle, a *quasmon*, which causes conditional probabilistic illusions. We discuss possible solid state implementations.

PACS numbers:

Transformation optics and metamaterials have made possible devices producing effects on wave propagation not seen in nature, including invisibility cloaks for electrostatics [1, 2], electromagnetism (EM) [3–5], acoustics [6–8] and quantum mechanics (QM) [9]; field rotators [10]; EM wormholes [11]; and illusion optics [12], among many others. The purpose of this paper is to give theoretical designs for devices, which we refer to as *Schrödinger hats*, acting as invisible concentrators, reservoirs and amplifiers for waves. Schrödinger hats exist for any wave phenomenon modeled by either the Helmholtz or Schrödinger equation, whether in EM, acoustics or QM. Schrödinger hats (SH) occupy one part of a parameter space continuum of wave-concentrating structures which also contains standard transformation optics based cloaks and cloaked sensors [13]. For EM and acoustic SH, the resulting centralized wave is a localized excitation, which may be super-wavelength in scale; in QM, the SH produces a new quasiparticle, a *quasmon*. Acoustic and EM Schrödinger hats require negative index materials, while highly oscillatory potentials are needed for QM hats. A SH seizes a large fraction of an incident wave, holding and amplifying it as a quasmon, while contributing only a negligible amount to scattering. These devices are consistent with the uncertainty principle, and we illustrate the concept by a QM version of three card monte. While a quantum Schrödinger hat is invisible to one-particle scattering, we show by effective potential theory [14] that a SH acts as an amplifier of two-particle Coulomb interactions. Such amplifiers may be useful for quantum measurement and information processing. The similar yet less demanding acoustic and EM hats offer equivalent effects, but existing metamaterials [15–18] make these designs more immediately realizable, allowing verification and further exploration of Schrödinger hats and quasmons.

There are a number of ‘paradoxes’ in which the laws of quantum mechanics imply results that conflict with our intuition [19]. In this spirit, here we show that the behavior of matter waves, as governed by Schrödinger’s equation, combined with the virtual space/physical space paradigm of transformation optics, allows one to manipulate conditional probabilities in QM and create quantum illusions, in which observed locations of particles differ from their actual values.

Ideal (perfect) 3D quantum invisibility cloaks at fixed energy  $E$  are based on the behavior of solutions to Schrödinger equations, with specific potentials and singular, inhomogeneous and anisotropic mass density [9]. These are mathematically equivalent, via a Liouville gauge transformation, to Helmholtz equations which also allow for cloaking in scalar optics [3, 20] and acoustics [7, 8, 21]. Realizing a QM cloak would be challenging, due to the extreme material parameters required [9]. We have previously described approximate QM cloaks, avoiding extreme and

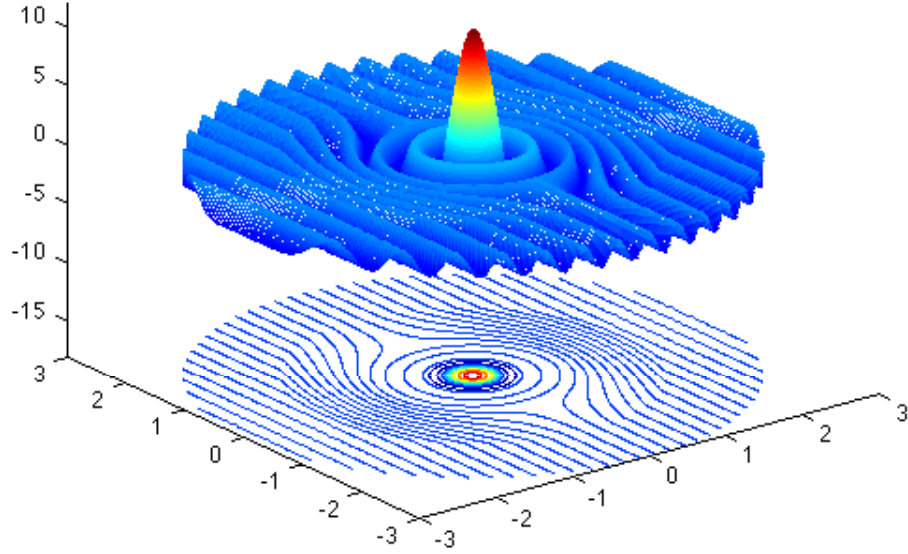


FIG. 1: **A quasmon inside a Schrödinger hat.** The real part of the effective wave function  $\psi_{eff}^{sh}(x, y, z)$  at the plane  $z = 0$  when a plane wave is incident to a SH potential. By varying the design parameters, the concentration of the wave inside the cloaked region can be made arbitrarily strong and the scattered field arbitrarily small. The matter wave is spatially localized, but conforms to the uncertainty principle, with the large gradient of  $\psi$ , visible as the steep slope of the central peak, concentrating the momentum in a spherical shell in  $p$ -space.

anisotropic parameters but nevertheless acting with arbitrary cloaking effectiveness [22, 23]. If a matter wave is incident to such a potential, the scattered wave can be made as small as desired. Analysis of approximate QM cloaks revealed a difficulty: the wave vanishes inside the cloak unless the cloak supports an almost trapped matter wave (or resonance), whose existence destroys the cloaking phenomenon and makes the ‘cloaked’ region in fact detectable. However, approximate cloaks can be tuned with a precise choice of parameters, *close to but not at* resonance; the flow of the wave from the exterior into the cloak and from the cloaked region out into the exterior are balanced, and the cloaking effect is not destroyed, but rather greatly improved [13]. We point out similar but surface-plasmon based effects [24] and other subwavelength plasmonics related to sensing [25, 26].

An approximate QM cloak can be implemented as follows, starting from the ideal 3D spher-

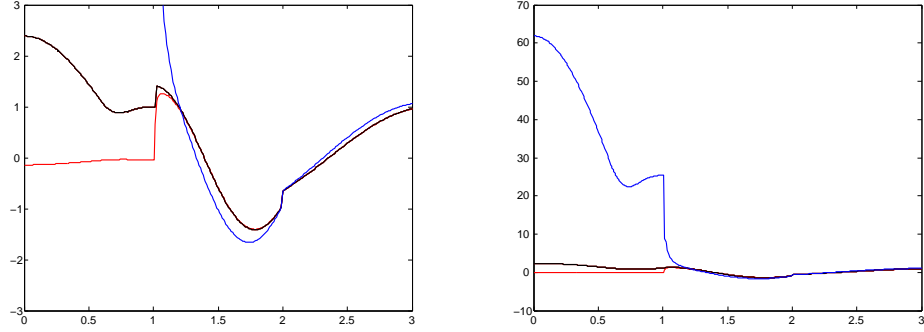


FIG. 2: **The cloak - resonance - Schrödinger hat continuum.** Scattering by potentials with different parameters, demonstrating three modes: cloak-, resonance- and Schrödinger hat-mode. The graphs show the real parts of the effective fields  $\psi^{eff}$  on  $0 < r < 3$ . The same curves are shown on different vertical scales: **(Left)** in  $[-3, 3]$ , illustrating the waves outside the cloak, and **(right)** in  $[-10, 70]$ , where the blow up inside the cloak can be seen. **(Red)** Quantum cloak (with parameter  $\tau_1 = \tau_1^{cl}$ ), for which incident wave does not penetrate the cloaked region. **(Blue)** Almost trapped wave ( $\tau_1 = \tau_1^{res}$ ). The cloaking effect is destroyed due to the strong resonance inside the cloak. **(Black)** Schrödinger hat ( $\tau_1 = \tau_1^{sh}$ ); probability mass is almost entirely captured by the cloaked region, yet scattering is negligible. The red and black curves are very close to the incident wave on  $r > 2$ , since both a cloak and a SH produce negligible scattering, while a resonant cloak is detectable in the far field. The discrepancy shown by the blue curve is due to the fact that resonances destroy cloaking and can be observed in the far field; with the parameters here, the difference in  $\psi^{eff}$  is small, but the destructive effect on cloaking can be much stronger. For parameters used, see discussion of numerical simulations in the Supplement.

ical transformation optics EM invisibility cloak [4]. This is based on the ‘blowing up a point’ coordinate transformation  $[1, 2] \mathbf{y} \mapsto \mathbf{x}$ ,

$$\mathbf{x} := F(\mathbf{y}) = \mathbf{y}, \text{ for } 2 < |\mathbf{y}| \leq 3; \quad F(\mathbf{y}) = \left(1 + \frac{|\mathbf{y}|}{2}\right) \frac{\mathbf{y}}{|\mathbf{y}|}, \text{ for } 0 < |\mathbf{y}| \leq 2. \quad (1)$$

This works equally well in acoustics, forming a cloak with a spherically symmetric singular anisotropic mass density and singular bulk modulus [7, 8, 21]. Consider the case where the anisotropic mass density,  $M(\mathbf{x})$ , is the identity matrix, and the inverse of the bulk modulus,  $\kappa(\mathbf{x})$ , is  $= 1$  outside the layer  $1 < r < 2$ ; the cloaked region is the ball  $B_1$  of radius 1 centered at

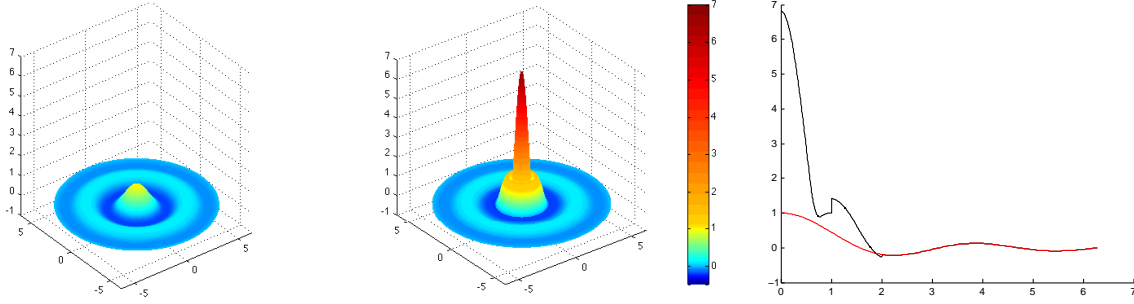


FIG. 3: **Quantum Three Card Monte.** The field  $\psi^{em}$  (**left**) and the effective field  $\psi_{eff}^{sh}$  (**center**) in the plane  $z = 0$  when particles are confined in a ball  $B_L$ . The central concentration of the wave function changes the conditional probabilities of the particles being found in regions in the vicinity of the cloak. (**Right**) The non-normalized probability densities  $|\psi^{em}|^2$  (**red**) and  $|\psi_{eff}^{sh}|^2$  (**black**) on the positive  $x$ -axis.

origin. For an arbitrary choice of  $R > 1$ , the ideal cloak is then approximated, replacing both the mass density and bulk modulus by 1 in the shell (or layer)  $1 < r < R$ . This gives a non-singular mass density  $M_R$  and non-singular bulk modulus  $\kappa_R^{-1}$ , which approach the ideal cloak parameters as  $R \searrow 1$ . Via homogenization theory, the anisotropic mass density  $M_R$  is approximable by *isotropic* mass densities  $m_\varepsilon$ , consisting of shells of thickness  $\varepsilon$  having alternating large and small densities, yielding a family of approximate cloaks [23]. One then obtains a QM cloak by applying the Liouville-gauge transformation  $\psi(\mathbf{x}) = m_\varepsilon^{-1/2}(\mathbf{x})u(\mathbf{x})$ , so that the Helmholtz equation becomes the time independent Schrödinger equation,  $(-\nabla \cdot \nabla + V_c - E)\psi = 0$ , where  $E = \omega^2$  is the energy and  $V_c = (1 - m_\varepsilon \kappa_R)E + m_\varepsilon^{1/2} \nabla \cdot \nabla (m_\varepsilon^{-1/2})$  is the cloaking potential for the energy level  $E$ .

For acoustic or EM cloaks constructed using positive index materials, resonances can allow large amounts of energy to be stored inside the ‘cloaked’ region, but at the price of destroying the cloaking effect [22, 23]. However, inserting negative index materials within the cloaked region allows for the cloaked storage of arbitrarily large amounts of energy; for simplicity, we describe this primarily in the context of QM cloaking, where the analogous effect is concentration of probability mass. When the cloaking potential is augmented by an internal potential consisting of a series of  $N$  shells, alternating positive barriers and negative wells with appropriately chosen parameters, the probability of the particle being inside the cloaked region can be made as close to 1 as desired. More precisely, insert into  $B_1$  a piecewise constant potential  $Q(\mathbf{x})$ , consisting of two shells, with

values  $\tau_1, \tau_2$ , in  $r \leq s_1, s_1 < r \leq s_2 < 1$ , resp., and zero elsewhere. For suitable parameters  $R, \epsilon, s_j$  and  $\tau_j$  of the potential  $W$ , we obtain, in the Supplement, a Schrödinger hat potential,  $V_{SH} = V_c + Q$ . Matter waves incident on the SH are modeled by Schrödinger's equation,

$$(-\nabla^2 + V_{SH} - E)\psi = 0. \quad (2)$$

The key feature of  $V_{SH}$  is that the matter waves governed by (2) can be made to concentrate inside the cloaked region as much as desired, while nevertheless maintaining the cloaking effect, quantified as follows. Assume that we have two balls of radius  $L > 2$ , one  $(B_L^{em})$  empty space and another  $(B_L^{sh})$  containing a Schrödinger hat. Let  $B_1, B_2$  denote the central balls of radii 1 and 2, resp., for  $\cdot = em$  or  $sh$ , and assume that matter waves  $\psi^{em}$  and  $\psi^{sh}$  on  $B_L^{em}, B_L^{sh}$ , resp., have the same boundary values on the sphere of radius  $L$ , corresponding to identical incident waves. Define the *strength* of the Schrödinger hat to be the ratio

$$\mathfrak{S} = \frac{1}{|\psi^{em}(0)|^2} \int_{B_1^{SH}} |\psi^{sh}(\mathbf{x})|^2 d\mathbf{x}.$$

where  $\psi^{em}(\mathbf{x})$  and  $\psi^{sh}(\mathbf{x})$  are solutions which coincide in  $|\mathbf{x}| > 2$ . We show that, by appropriate choice of the design parameters,  $\mathfrak{S}$  may be made to take any prescribed positive value. For large values of  $\mathfrak{S}$ , the probability mass of  $\psi^{sh}$  is almost completely concentrated in the cloaked region. For  $\varepsilon > 0$ , the wave  $\psi^{sh}$  is rapidly oscillating, and so we also consider the effective wave,  $\psi_{eff}^{sh}$ , which is obtained as the limit of  $\varepsilon \rightarrow 0$  (in a suitable weak sense discussed in the Supplement). This is distinct from the ‘mirage effect’ for standard cloaks, which makes a source within the cloaking layer appear to be in a different position due to the chain rule [20, 27].

We next describe some remarkable properties of Schrödinger's hat. To start with, the highly concentrated part of the wave function which the SH and the incident wave produce inside the cloaked region can be considered as a quasiparticle, which we call a *quasmon*. A quasmon has a well-defined electric charge and variance of momentum depending on the parameters of  $V_{SH}$ . Secondly, the amplification and concentration of a matter wave in the cloaked region can be used to create probabilistic illusions. Consider (non-normalized) wave functions  $\psi^{em}$  and  $\psi^{sh}$  which coincide in  $B_L - B_2$ , i.e., exterior to the cloaking structure. Then for any region  $R_{out}$  in  $B_L - B_2$  the conditional probability that the particle is observed to be in  $R_{out}$ , given that it is observed in  $B_L - B_2$ , is the same for  $\psi^{em}$  and  $\psi^{sh}$ . However, by choosing the parameters of the SH appropriately (see the Supplement), the probability that the particle is in the cloaked region  $B_1$  can be made as close to 1 as wished. Roughly speaking, the particle  $\psi^{sh}$  is like a trapped ghost

of the particle  $\psi^{em}$  in that it is located in the exterior of the cloaking structure with far lower probability than  $\psi^{em}$  is, but when  $\psi^{sh}$  is observed in  $B_L - B_2$ , all measurements coincide with those of  $\psi^{em}$ . When a particle is close to a  $SH$ , with a large probability it is grasped by the hat and bound into storage within the cloaked region as a quasmon. This is nevertheless consistent with the uncertainty principle: although the particle is spatially localized within  $B_1$ , the expected value of the magnitude of its momentum is large, due to the large gradient of  $\psi^{sh}$  on a spherical shell about the central peak; cf. Figs. 1 & 3(center, right).

The Schrödinger hat produces vanishingly small changes in the matter wave outside of the cloak, while simultaneously making the particle concentrate inside the cloaked region. Thus, if the matter wave is charged, it may couple via Coulomb interaction with other particles or measurement devices external to the cloak. When an incident field  $\psi^{in}$  is scattered by the  $SH$ , the wave field is not perturbed outside of the support of the hat potential  $V_{SH}$ ; there are no changes in scattering measurements. However, the cloak concentrates the charge inside the cloaked region, proportional to the square of the modulus of the value  $\psi^{in}(O)$  which the incident field would have had at the center  $O$  of  $B_L^{em}$  in the absence of the  $SH$ . Due to the long range nature of the Coulomb potential, this charge causes an electric field which may be strong even far away from the  $SH$ . If one measures the electric field and the result is zero, then this indicates that  $\psi^{in}(O) = 0$ ; without disturbing the field, one determines whether the incident field vanishes at a given point. A measuring device within a Schrödinger hat thus acts as a non-interacting sensor, detecting the nodal curves or surfaces on which the incident matter field  $\psi^{in}$  vanishes, an effect analogous to cloaked acoustic and EM sensors [13, 24] and near-field scanning optical microscopes [28]. As described in the Supplement, a Schrödinger hat potential also amplifies the interaction between two charged particles.

The behavior of Schrödinger hats and quasmons can be illustrated by means of a quantum variant of Three Card Monte, the classic game of chance in which a coin is hidden under one of three bowls and the player guesses where the coin is. Consider first a preliminary version of the game, played by Alice, who runs the game, and Bob, who makes the guesses. In place of bowls, they play the game using  $N$  empty balls, each a copy of  $B_L^{em}$ , and the coin is replaced by a QM particle. The surface of each ball is made of material representing an infinite potential wall, so that a particle within cannot escape; this corresponds to the Dirichlet boundary condition on the boundary. In the game, Alice inserts one particle into one of the balls, after which she mixes the balls randomly and asks Bob to guess in which ball the particle is. Bob chooses one and makes

internal measurements near the boundary of  $B_L$ . Bob, wishing to determine whether the particle is in a region  $R$ ,  $R \subseteq B_L - B_2$ , measures the value of an observable  $A$ , which is 1 if the particle is observed ( $X \in R$ ) and 0 otherwise; the value of  $A$  is also 0 if the particle is not in the chosen ball. The expected value of  $A$  is  $p \cdot \mu_A^{em} + (1 - p) \cdot 0 = p \cdot \mu_A^{em}$ . Here,  $p = 1/N$  is the probability that Bob chose the ball that into which Alice inserted the particle, and  $\mu_A^{em} = a_{em}/c_{em}$ , where  $a_{em} = \int_R |\psi^{em}(\mathbf{x})|^2 d\mathbf{x}$ ,  $c_{em} = \|\psi^{em}\|_{L^2(B_L)}^2$ , and  $\psi^{em}$  is the empty space wave function on  $B_L^{em}$ .

To make the game more interesting, Alice and Bob make a wager: they agree that Bob will pay  $p\mu_A^{em} \text{ €}$  to Alice in advance of each turn, but if he then observes a particle will receive 1 € back from Alice. With these rules, the game is fair, with expected profit 0 for both Alice and Bob.

Now suppose that, before play commences, and unbeknownst to Alice and Bob, a third player (the Cloaker) replaces each of the  $N$  empty balls with a ball  $B_L^{sh}$  equipped with a Schrödinger hat. The expectation of  $A$  is now  $p \cdot \mu_A^{sh} + (1 - p) \cdot 0 = p \cdot \mu_A^{sh}$ , where  $\mu_A^{sh} = a_{sh}/c_{sh}$ , where  $a_{sh} = \int_R |\psi^{sh}(\mathbf{x})|^2 d\mathbf{x}$ ,  $c_{sh} = \|\psi^{sh}\|_{L^2(B_L)}^2$ , and  $\psi^{sh}$  is the wave function on  $B_L^{sh}$ .

Since a Schrödinger hat is an effective cloak,  $\psi^{em} = \psi^{sh}$  outside of the ball  $B_2$  which contains  $R$ , and so  $a_{em} = a_{sh}$ . On the other hand, the presence of the Schrödinger hat amplifies the wave function in  $B_1^{sh}$  and so  $c_{sh} \gg c_{em}$ ; hence  $\mu_A^{sh} \ll \mu_A^{em}$ , cf. Fig. 3. When the game is played many times, Bob's expected chance of observing the particle in the ball which he chose is smaller than it was before the Schrödinger hats were inserted. In other words, after the Cloaker's intervention the particles start to disappear from Bob's observations and Bob starts to lose; Alice is unknowingly 'cheating'. The game can be made as unfair as one wishes by choosing parameters so that  $\mathfrak{S}$  is very large, using general Schrödinger hat potentials as described in the Supplement.

We conclude by describing one possible path, discussed in more detail at the end of the paper, towards a solid state realization of a quantum Schrödinger hat, utilizing a sufficiently large heterostructure of semiconducting materials. By homogenization theory, the SH potential can be approximated using layered potential well shells of depth  $-V_-$  and wall shells of height  $V_+$ . By rescaling the  $x$  coordinate we can make the values  $V_{\pm}$  smaller (note that in such scaling the size of the support of the SH potential grows and  $E$  becomes smaller). This sequence of spherical potential walls and wells can be implemented using a heterostructure of semiconducting materials. In such a structure the wave functions of electrons with energy close to the bottom of the conduction bands can be approximated using Bastard's envelope function method [29]. Choosing the materials and thickness of the spherical layers suitably, the envelope functions then satisfy a Schrödinger equation whose solutions are close to those corresponding to the SH potential.



# Supplemental Material

**In this supplement, we provide the rigorous analysis needed to confirm the existence and behavior of Schrödinger hats, specify the parameters used in the Figures, and detail the proposed solid-state implementation.**

## ANALYSIS OF QUANTUM CLOAKS AND SCHRÖDINGER HAT POTENTIALS

### An approximate acoustic cloak

Below we will use the approximate cloaks modeled by the Helmholtz (or the Schrödinger) type equation

$$\begin{aligned} (-\nabla \cdot M_R^{-1} \nabla - \omega^2 \kappa_R) u_R &= 0 \quad \text{in the domain } \Omega \subset \mathbb{R}^3, \\ u_R &= h \quad \text{on the boundary } \partial\Omega, \end{aligned} \tag{3}$$

where  $R > 1$  is a parameter corresponding to the effectiveness of the cloak,  $\omega$  is the frequency, and  $M_R$  and  $\kappa_R$  are the coefficient functions defined below. Let  $\nu$  denote the outward unit normal vector of  $\partial\Omega$ . Measurements on the boundary  $\partial\Omega$  are mathematically modeled by the Dirichlet-to-Neumann operator defined by

$$\Lambda_R(h) = \nu \cdot M_R^{-1} \nabla u_R|_{\partial\Omega},$$

describing the response of the system, i.e., the Neumann boundary value  $\nu \cdot M_R^{-1} \nabla u_R|_{\partial\Omega}$ , when the Dirichlet data  $u_R = h$  is posed on the boundary. In the theory of the approximate cloaks the coefficient functions  $M_R$  and  $\kappa_R$  are constructed in such a way that as  $R \searrow 1$  the Dirichlet-to-Neumann operators  $\Lambda_R$  approach to the Dirichlet-to-Neumann operator  $\Lambda^{homog} : h \mapsto \nu \cdot \nabla u|_{\partial\Omega}$  for the boundary value problem

$$\begin{aligned} (-\nabla \cdot \nabla - \omega^2) u &= 0 \quad \text{in the domain } \Omega \subset \mathbb{R}^3, \\ u_R &= h \quad \text{on the boundary } \partial\Omega, \end{aligned} \tag{4}$$

modeling empty space. In practical terms, this means that when the parameter  $R$  is close to 1, for the approximative cloak all boundary observations on  $\partial\Omega$  are close to the observations on  $\partial\Omega$  made when the domain  $\Omega$  is filled with a homogeneous, isotropic medium.

Approximate cloaks are the basis of our construction of Schrödinger hat potentials. We start by recalling some facts concerning nonsingular approximations to ideal 3D spherical cloaks [22, 23, 30–33]. For  $R > 0$ , let  $B_R = \{|\mathbf{x}| < R\}$  and  $S_R = \{|\mathbf{x}| = R\}$  be the open ball and sphere, resp., centered at the origin  $\mathcal{O}$  and of radius  $R$  in three-space. Moreover, let  $\overline{B}_R = \{|\mathbf{x}| \leq R\}$  be the closed ball. For  $1 \leq R < 2$ , set  $\rho = 2(R - 1)$ ,  $0 \leq \rho < 2$ , so that  $R \searrow 1$  as  $\rho \searrow 0$ , and introduce the coordinate transformation  $F_R : B_L - B_\rho \rightarrow B_L - B_R$ ,

$$\mathbf{x} := F_R(\mathbf{y}) = \begin{cases} \mathbf{y}, & \text{for } 2 < |\mathbf{y}| < L, \\ \left(1 + \frac{|\mathbf{y}|}{2}\right) \frac{\mathbf{y}}{|\mathbf{y}|}, & \text{for } \rho < |\mathbf{y}| \leq 2. \end{cases} \quad (5)$$

For  $R = 1$  ( $\rho = 0$ ), this is the singular transformation of [1, 2, 4], leading to the ideal transformation optics cloak, while for  $R > 1$  ( $\rho > 0$ ),  $F_R$  is nonsingular and leads to a class of approximate cloaks [22, 23, 30, 32, 33]. Thus, if  $M_0 \equiv \delta_{jk}$  denotes the homogeneous, isotropic mass tensor, then, for  $R = 1$ , the transformed tensor becomes an anisotropic singular mass tensor,  $M_{1,jk}(\mathbf{x})$ , on  $1 < |\mathbf{x}| < L$ , defined in terms of its inverse,

$$(M_1^{-1})^{jk}(\mathbf{x}) = ((F_1)_*\delta)^{jk}(\mathbf{y}) := \frac{1}{\det[\frac{\partial F_1}{\partial x}(\mathbf{x})]} \sum_{p,q=1}^3 \frac{\partial(F_1)^j}{\partial x^p}(\mathbf{x}) \frac{\partial(F_1)^k}{\partial x^q}(\mathbf{x}) \delta^{pq}(\mathbf{x}) \Big|_{\mathbf{x}=F_1^{-1}(\mathbf{y})}. \quad (6)$$

This means that in the Cartesian coordinates  $M_1(\mathbf{x})$  is the matrix with elements

$$(M_1)_{jk}(\mathbf{x}) = \frac{1}{2}(\delta_{jk} - P_{jk}(\mathbf{x})) + \frac{1}{2}(|\mathbf{x}| - 1)^{-2} P_{jk}(\mathbf{x}), \quad 1 < |\mathbf{x}| < 2,$$

where the matrix  $P(\mathbf{x})$ , having elements  $P_{jk}(x) = |\mathbf{x}|^{-2} x_j x_k$ , is the projection to the radial direction.

On the other hand, when  $R > 1$ , we obtain an anisotropic but nonsingular mass tensor,  $M_{R,jk}(\mathbf{x})$ , on  $R < |\mathbf{x}| < L$ , given by

$$(M_R^{-1})^{jk}(\mathbf{x}) = ((F_R)_*\delta)^{jk}(\mathbf{y}) := \frac{1}{\det[\frac{\partial F_R}{\partial x}(\mathbf{x})]} \sum_{p,q=1}^3 \frac{\partial(F_R)^j}{\partial x^p}(\mathbf{x}) \frac{\partial(F_R)^k}{\partial x^q}(\mathbf{x}) \delta^{pq}(\mathbf{x}) \Big|_{\mathbf{x}=F_R^{-1}(\mathbf{y})}. \quad (7)$$

For each  $R > 1$ , the eigenvalues of  $M_R$  are bounded from above and below; however, two of them  $\nearrow \infty$  as  $R \searrow 1$ . We define an approximate mass tensor  $M_R$  everywhere on  $B_L$  by extending it as an identity matrix,

$$M_{R,jk}^{ext}(\mathbf{x}) = \begin{cases} M_{R,jk}(\mathbf{x}) & \text{for } R < |\mathbf{x}| \leq 2, \\ \delta_{jk}, & \text{for } |\mathbf{x}| < R \text{ or } 2 < |\mathbf{x}| \leq L. \end{cases} \quad (8)$$

In sequel, we use the notation  $M_{R,jk}(\mathbf{x})$  also for  $M_{R,jk}^{ext}(\mathbf{x})$ . We define a scalar function  $\kappa_R(\mathbf{x})$  on  $B_L$ ,

$$\kappa_R(\mathbf{x}) = \begin{cases} \eta(\mathbf{x}), & \text{for } |\mathbf{x}| \leq R_0, \\ 64|\mathbf{x}|^{-4}(|\mathbf{x}| - 1)^4 & \text{for } R < |\mathbf{x}| < 2, \\ 1, & \text{for } R_0 \leq |\mathbf{x}| \leq R \text{ or } 2 \leq |\mathbf{x}| \leq L. \end{cases} \quad (9)$$

where

$$\eta(\mathbf{x}) = \eta(\mathbf{x}; \tau) = \sum_{j=1}^N \tau_j \chi_{(s_{j-1}, s_j)}(|\mathbf{x}|). \quad (10)$$

Here  $\tau = (\tau_1, \tau_2, \dots, \tau_N)$ ,  $\tau_j \in \mathbb{R}$  are parameters which one can vary,  $0 = s_0 < s_j < s_N = R_0$  are some fixed numbers, and  $\chi_{(s_{j-1}, s_j)}(r)$  is the indicator function of the interval  $(s_{j-1}, s_j)$ . This means that we have a homogeneous ball  $B_{s_0}$  coated with homogeneous shells. Sometimes we denote  $\kappa_R(\mathbf{x}) = \kappa_R(\mathbf{x}; \tau)$ . Note that in acoustics  $\kappa_R$  has the meaning of inverse of bulk modulus; later, in quantum mechanics, it gives rise to the potential.

Below, we consider what happens as  $R \searrow 1$ . In fact, for rigorous mathematical analysis we should modify the above definition of  $\kappa_R$  by replacing it, e.g., by  $\kappa_1$  so that for all  $x \in B_L$  the quadratic form corresponding to operator  $\int_{B_L} (\nabla v \cdot M_R^{-1} \nabla \bar{v} - \omega^2 \kappa_R |v|^2) d\mathbf{x}$  becomes smaller (for any fixed  $v$ ) as  $R$  decreases. However, in order to compute solutions explicitly and to present considerations in a simplified way, we will consider the case when  $\kappa_R$  is defined as above. Mathematical proofs will be presented elsewhere.

Next, consider in the domain  $B_L$  the solutions of the Dirichlet problem,

$$(-\nabla \cdot M_R^{-1} \nabla - \omega^2 \kappa_R) u_R = 0 \quad \text{in } B_L, \quad u_R|_{S_L} = h. \quad (11)$$

Since, for  $1 < R < 2$ , the matrix  $M_R$  is nonsingular everywhere, across the internal interface  $S_R$  we have the standard transmission conditions,

$$\begin{aligned} u_R|_{S_{R+}} &= u_R|_{S_{R-}}, \\ \mathbf{e}_r \cdot (M_R^{-1} \nabla u_R)|_{S_{R+}} &= \mathbf{e}_r \cdot (M_R^{-1} \nabla u_R)|_{S_{R-}}, \end{aligned} \quad (12)$$

where  $\mathbf{e}_r$  is the radial unit vector and  $\pm$  indicates the trace on  $S_R$  as  $r \rightarrow R^\pm$ .

In the physical space  $B_L$  one has

$$u_R(\mathbf{x}) = \begin{cases} v_R^+(F_R^{-1}(\mathbf{x})), & \text{for } R < |\mathbf{x}| < L, \\ v_R^-(\mathbf{x}), & \text{for } |\mathbf{x}| \leq R, \end{cases} \quad (13)$$

with  $v_R^\pm$  in the virtual space, which consists of the disjoint union  $(B_L - B_\rho) \cup B_R$ , satisfying

$$\begin{aligned} (-\nabla^2 - \omega^2)v_R^+(\mathbf{y}) &= 0 \quad \text{for } \rho < |\mathbf{y}| < L, \\ v_R^+|_{S_L} &= h, \end{aligned}$$

and

$$(-\nabla^2 - \omega^2 \kappa_R)v_R^-(\mathbf{y}) = 0, \quad \text{for } |\mathbf{y}| < R. \quad (14)$$

With respect to spherical coordinates  $(r, \theta, \phi)$ , the transmission conditions (12) become

$$\begin{aligned} v_R^+(\rho, \theta, \phi) &= v_R^-(R, \theta, \phi), \\ \rho^2 \partial_r v_R^+(\rho, \theta, \phi) &= R^2 \partial_r v_R^-(R, \theta, \phi). \end{aligned} \quad (15)$$

Since  $M_R, \kappa_R$  are spherically symmetric, cf. (8,9), we can separate variables in (11), representing  $u_R$  as

$$u_R(r, \theta, \phi) = \sum_{n=0}^{\infty} \sum_{m=-n}^n u_R^{nm}(r) Y_n^m(\theta, \phi), \quad (16)$$

where  $Y_n^m$  are the standard spherical harmonics. Then equations (11) give rise to a family of boundary value problems for the  $u_R^{nm}$ . For our purposes, the most important one is the lowest harmonic term (the  $s$ -mode),  $u_R^{0,0}$ , i.e., the radial component of  $u_R$ , which is independent of  $(\theta, \phi)$ . This is studied in the next section.

### Spherical harmonic coefficients

**The lowest harmonics.** For  $R_0 < 1 < R < 2$ , consider the Dirichlet problem on the ball  $B_L$ ,

$$\begin{aligned} (-\nabla \cdot M_R^{-1} \nabla - \omega^2 \kappa_R)u_R &= 0 \quad \text{in } B_L, \\ u_R|_{S_L} &= h(\mathbf{x}). \end{aligned} \quad (17)$$

We will express asymptotics in terms of the quantity  $\rho = 2(R - 1)$  as  $\rho \searrow 0$ .

We have shown elsewhere [23] that

- For a specific value of the parameter  $\tau \in \mathbb{R}^N$ , denoted  $\tau = \tau^{res}(R, \omega)$ , there is a blow-up effect, or interior resonance, destroying cloaking. This corresponds to the case when  $\tau$  is such that there equation (17) has a non-zero radial solution with  $h = 0$ . In this case the

solution  $u_R$  grows very much inside the cloaked region as  $R \rightarrow 1$ . This means that the inside of the cloak is in resonance and the wave tunnels outwards through the cloak, so that this resonance is detected by boundary measurements outside of the cloak.

- For another specific value of  $\tau$ , denoted  $\tau = \tau^{sen}(R, \omega)$ , the cloak acts as an approximate cloak and inside the cloaked region the solution is proportional to the value which the field in the empty space would have at the origin. This corresponds to the case when the equation (17) has a radial solution  $u_R$  which satisfies  $\partial_r u_R(L) = \omega j'_0(\omega L)$  and  $u_R(L) = j_0(\omega L)$ , or equivalently,  $u_R(\mathbf{x}) = j_0(\omega |\mathbf{x}|)$  for  $R < |\mathbf{x}| < L$ .

Due to the transmission condition (12) we see that the values  $\tau^{res}(R, \omega)$  and  $\tau^{sen}(R, \omega)$  are close and  $\lim_{R \rightarrow 1} \tau^{sen}(R, \omega) = \lim_{R \rightarrow 1} \tau^{res}(R, \omega)$ .

We now explain in detail how to choose  $\tau = \tau^{sen}(R, \omega)$ : First, fix  $R$  and  $\omega$ , and choose  $0 < R_0 < 1$ . Consider the ordinary differential equation corresponding to the radial solutions  $u(r)$  of the equation (17), that is,

$$-\frac{1}{r^2} \frac{d}{dr} \left( r^2 \sigma_R(r) \frac{d}{dr} u(r) \right) - \omega^2 \kappa_R(r) u(r) = 0, \quad (18)$$

and pose the Cauchy data (i.e. initial data) at  $r = L$ ,  $u(L) = j_0(L\omega)$ ,  $\partial_r u(L) = \omega j'_0(L\omega)$ . Here,  $\sigma_R(r)$  is the  $rr$ -component of the matrix  $M_R^{-1}$ , that is,  $\sigma_R(r) = 2(r-1)^2$ , for  $R < r < 2$  and  $\sigma_R(r) = 1$ , elsewhere. Then we solve the initial value problem for the ordinary differential equation (18) on interval  $r \in [R_0, L]$  and find the Cauchy data  $(u(R_0), \frac{du}{dr}(R_0))$  at  $r = R_0$ . Note that on the interval  $r \in [R_0, L]$ ,  $\kappa_R$  does not depend on  $\tau$ . Consider next the case when

$$N = 2, \quad s_1 = R_0/2, \quad s_2 = R_0, \quad \tau = (\tau_1, \tau_2), \quad (19)$$

where  $\tau_1$  and  $\tau_2$  are constructed in the following way:

First, we choose  $\tau_2$  to be a negative number with a large absolute value. We then solve of the initial value problem for (18) on interval  $r \in [s_1, R_0]$  with initial data  $(u(R_0), \frac{du}{dr}(R_0))$  at  $r = R_0$ . In particular, this determines the Cauchy data  $(u(s_1), \frac{du}{dr}(s_1))$  at  $r = s_1$ .

Secondly, consider  $\tau_1, \tau_2$ , as well as  $R, R_0$ , to be parameters, and solve the initial value problem for (18) on interval  $r \in [0, s_1]$  with initial data  $(u(s_1), \frac{du}{dr}(s_1))$  at  $r = s_1$ . Denote the solution by  $u(r; \tau_1, R, R_0, \tau_2)$  and find the value  $\frac{du}{dr}(r; \tau_1, R, R_0, \tau_2)|_{r=0}$ . Then, for given  $R, R_0$ , and  $\tau_2$ , we find  $\tau_1 > 0$  satisfying

$$\frac{du}{dr}(0; \tau_1, R, R_0, \tau_2) = 0. \quad (20)$$

We choose  $\tau_1$  to be the smallest value for which (20) holds, and denote this solution by  $\tau_1(R, R_0, \tau_2)$ . Summarizing the above computations, we have obtained a cloak at the frequency  $\omega$ , that is, for the energy  $E_0 = \omega^2$ , such that its radial solution  $u(\mathbf{x})$  satisfies  $u(\mathbf{x}) = j_0(\omega|\mathbf{x}|)$  for  $|\mathbf{x}| \in [2, L]$ . Moreover, when  $\tau_2$  is large, this solution  $u_R(r)$  grows exponentially fast on the interval  $[s_1, s_2]$ , as  $r$  becomes smaller, while on the interval  $[0, s_1]$  it satisfies  $\frac{du_R}{dr}(0) = 0$ , so that  $u(r)$  defines a smooth spherically symmetric solution of (17).

In the context of QM cloaks below, the construction above can be considered as follows: Inside the cloak there is a potential well of the depth  $\tau_1$ , enclosed by a potential wall having the height  $\tau_2$ . The parameters  $\tau_1$  and  $\tau_2$  are chosen so that the solution is large inside the cloak due to the resonance there. Moreover, the choice of the parameters is such that the flow associated to the wave function from the outside into the cloaked region and from the cloaked region to the outside are in balance. The cloaked region is thus well-hidden even though the solution may be very large inside the cloaked region. In a scattering experiment, with high probability the potential captures the incoming particle, but due to the chosen parameters of the cloak, external measurements cannot detect this.

Using the implicit function theorem, one can show that for generic values of  $\tau_2$  and  $R_0$ , there is a limit  $\lim_{R \searrow 1} \tau_1(R, R_0, \tau_2) = \tau_1(R_0, \tau_2)$ . We note that the solution  $u_R(r) = u(r; \tau_1(R, R_0, \tau_2), R, \tau_2)$  of (18) has limit  $\lim_{R \searrow 1} u(r; \tau_1(R, R_0, \tau_2), R, \tau_2) = c\Phi(r)$ ,  $r < 1$ , where  $c \in \mathbb{C}$  and  $\Phi(r) \not\equiv 0$  an eigenfunction of the boundary value problem

$$\begin{aligned} (\nabla^2 + \omega^2 \kappa_1(\mathbf{y}; \tau))\Phi(\mathbf{y}) &= 0, \quad \text{for } |\mathbf{y}| < 1, \\ \partial_r \Phi(\mathbf{y})|_{r=1} &= 0, \end{aligned} \tag{21}$$

where  $\tau = (\tau_1(1, R_0, \tau_2), \tau_2)$  and  $\Phi$  is normalized so that  $\|\Phi\|_{L^2(B_1)} = 1$ .

**Higher order harmonics.** Let  $\tau = (\tau_1(R_0, \tau_2), \tau_2)$ . As  $\tau_1$  was chosen to be the smallest solution of (20) we have that  $\omega$  an eigenfrequency of the problem

$$\begin{aligned} (-\nabla^2 - \omega^2 \kappa_1(r; \tau))v(\mathbf{y}) &= 0, \quad \text{for } |\mathbf{y}| < 1, \\ \partial_r v(\mathbf{y})|_{r=1} &= 0. \end{aligned} \tag{22}$$

Let us now analyze the solution (13) using spherical harmonics. Recall that in  $B_R$  the function  $v_R^-(\mathbf{y}) = u_R(\mathbf{y})$  is a solution to the homogeneous equation (14). Thus, in particular,

$$v_R^-(r, \theta, \varphi) = \sum_{n=0}^{\infty} \sum_{m=-n}^n u_R^{nm}(r) Y_n^m(\theta, \varphi), \tag{23}$$

where

$$\begin{aligned} u_R^{nm}(r) &= a_{nm}j_n(\omega r) + p_{nm}h_n^{(1)}(\omega r), \quad R_0 < r < R, \\ u_R^{nm}(r) &= \hat{a}_{nm}j_n(\omega\sqrt{\tau_2}r) + \hat{p}_{nm}h_n^{(1)}(\omega\sqrt{\tau_2}r), \quad R_0/2 < r \leq R_0, \\ u_R^{nm}(r) &= \tilde{a}_{nm}j_n(\omega\sqrt{\tau_1}r), \quad 0 < r \leq R_0/2, \end{aligned} \quad (24)$$

and  $\sqrt{\tau_2}$  is pure imaginary. Here  $\tilde{a}_{nm} = \tilde{a}_{nm}(\omega; R)$ ,  $a_{nm} = a_{nm}(\omega; R)$ ,  $p_{nm} = p_{nm}(\omega; R)$  etc. are yet undefined coefficients. Note that the terms with  $h_n^{(1)}(\omega\sqrt{\tau_1}r)$  are absent near  $r = 0$  since  $v_R^-(\mathbf{y})$  has no singularity at 0.

Now, for  $\rho < r < L$ ,

$$v_R^+(r, \theta, \varphi) = \sum_{n=0}^{\infty} \sum_{m=-n}^n (c_{nm}h_n^{(1)}(\omega r) + b_{nm}j_n(\omega r))Y_n^m(\theta, \varphi),$$

with as yet unspecified  $b_{nm} = b_{nm}(\omega; R)$  and  $c_{nm} = c_{nm}(\omega; R)$ .

Expand the boundary value  $h$  on  $\partial B_L$  in surface spherical harmonics as

$$h(\theta, \varphi) = \sum_{n=0}^{\infty} \sum_{m=-n}^n f_{nm}Y_n^m(\theta, \varphi). \quad (25)$$

As shown in the previous section,  $b_{00} = f_{00}$ ,  $c_{00} = 0$ , and both  $p_{00}$  and  $a_{00}$  can be solved for using the transmission conditions, which determines the coefficients for  $n = 0$ .

Next we consider the higher-order coefficients, for  $n \geq 1$ . To simplify notations, denote by  $U_R^{nm}(r)Y_n^m(\theta, \varphi)$  the solution of (14) for which  $U_R^{nm}(r) = j_n(\omega\sqrt{\tau_1}r)$  for  $r < R_0/2$ . Then the coefficients in (23) can be written in the form  $u_R^{nm}(r) = \tilde{a}_{nm}U_R^{nm}(r)$ . Observe that there exist the limit

$$\lim_{R \rightarrow 1} U_R^{nm}(r) = U_1^{nm}(r)$$

and due to the way the coefficient  $\tau_1 = \tau_1(R_0, \tau_2)$  was chosen, for generic values of  $\tau_2$  we have

$$\partial_r U_1^{nm}(1) \neq 0 \text{ for all } n \geq 1, -n \leq m \leq n. \quad (26)$$

Next we assume that  $\tau_2$  is such that (26) holds.

By the transmission condition (12),

$$\begin{aligned} \tilde{a}_{nm}(R)U_R^{nm}(R) &= b_{nm}(R)j_n(\omega\rho) + c_{nm}(R)h_n^{(1)}(\omega\rho), \\ R^2\tilde{a}_{nm}(R)\partial_r U_R^{nm}(r)|_{r=R} &= \rho^2 b_{nm}(R)\partial_r j_n(\omega r)|_{r=\rho} + c_{nm}(R)\partial_r h_n^{(1)}(\rho)|_{r=\rho}. \end{aligned} \quad (27)$$

Using asymptotics of Bessel and Hankel functions [34], we obtain from (27) that

$$\begin{aligned} c_{nm}(R) &= \frac{2^n n!}{(2n+1)(2n)!} \tilde{a}_{nm}(R) \partial_r U_1^{nm}(1) \omega^{n+1} \rho^n + O(\rho^{n+1}), \\ b_{nm}(R) &= -\frac{(2n)!}{2n!} \tilde{a}_{nm}(R) \partial_r U_1^{nm}(1) \omega^{-n} \rho^{-(n+1)} + O(\rho^{-n}). \end{aligned} \quad (28)$$

Note that above  $\partial_r U_1^{nm}(1)$  is non-vanishing by (26). Using (28) and the Dirichlet condition (25), we finally see that

$$\tilde{a}_{nm}(R) = (2n+1) \alpha_n f_{nm} \omega^n \frac{1}{j_n(\omega L)} \rho^{n+1} + O(\rho^{n+2}). \quad (29)$$

Together with the transmission conditions on  $r = R_0$  and  $r = R_0/2$ , this implies that

$$\begin{aligned} b_{mn} &= \frac{1}{j_n(L\omega)} f_{mn} + O(\rho), \quad c_{mn} = O(\rho^{2n+1}), \\ a_{mn}, \hat{a}_{nm}, \tilde{a}_{nm} &= O(\rho^{n+1}), \quad p_{mn}, \hat{p}_{nm} = O(\rho^{n+1}). \end{aligned} \quad (30)$$

The above considerations for  $n = 0$  and for  $n \geq 1$  can be summarized as follows: As  $R \searrow 1$ , the solutions  $u^R(\mathbf{x})$  converge in  $B_L - B_2$  to the solution  $u$  corresponding to the homogeneous virtual space,

$$\begin{aligned} (-\nabla \cdot \nabla - \omega^2)u &= 0 \quad \text{in } B_L \\ u|_{S_L} &= h(\mathbf{x}) \end{aligned} \quad (31)$$

and, in the domain  $B_1$ , to the solution in empty space,

$$\lim_{R \rightarrow 1} u^R(\mathbf{x}) = \beta u(0) \Phi(\mathbf{x}) \quad (32)$$

where  $\Phi(\mathbf{y}) = \Phi(r)$  is the radial solution of the equation (22),  $\beta = \frac{1}{\Phi(1)}$  and  $u(0)$  is the value of the solution of (31) at the origin.

Next we consider the implications of this for quantum mechanics.

### Approximate isotropic cloaks in quantum mechanics - Schrödinger's hat potential

The approximate anisotropic cloak  $(M_R, \kappa_R)$  can be further approximated by an isotropic cloak  $(m_{R,\varepsilon}, \kappa_R)$ , where  $m_{R,\varepsilon}(\mathbf{x})$  is a smooth isotropic (i.e., scalar-valued) mass density, which we denote by lowercase  $m$  to distinguish it from the anisotropic mass tensor denoted by  $M$ . It satisfies  $C_1(R, \varepsilon) > m_{R,\varepsilon}(\mathbf{x}) > c_1 > 0$ , and leads to an approximate cloak equation,

$$\begin{aligned} \left( -\nabla \cdot \frac{1}{m_{R,\varepsilon}} \nabla - \omega^2 \kappa_R \right) u_{R,\varepsilon} &= 0 \quad \text{in } B_L \\ u_{R,\varepsilon}|_{S_L} &= h(\mathbf{x}). \end{aligned} \quad (33)$$



We will use isotropic mass densities which, for  $R < |\mathbf{x}| < 2$ , are of the form

$$\frac{1}{m_{R,\varepsilon}(\mathbf{x})} = a(|\mathbf{x}|)p_1\left(\frac{|\mathbf{x}| - R}{\varepsilon}\right) + b(|\mathbf{x}|)p_2\left(\frac{|\mathbf{x}| - R}{\varepsilon}\right) + p_3\left(\frac{|\mathbf{x}| - R}{\varepsilon}\right). \quad (34)$$

Here,  $p_1, p_2, p_3$  are bounded non-negative smooth functions with period one such that  $p_1, p_2 = 0$  near integer values, while  $p_3 = 1$  near integer values. For each  $\rho > 0$  we choose a sequence of  $\varepsilon_k = \varepsilon_k(\rho) \rightarrow 0$  as  $k \rightarrow \infty$  such that  $\frac{2-R}{\varepsilon_k(\rho)}$  is an integer. As for  $|\mathbf{x}| \leq R$  and  $|\mathbf{x}| \geq 2$ , we take  $m_{\rho,\varepsilon}(\mathbf{x}) = 1$ . It is possible to choose  $a(|\mathbf{x}|) = O(1)$  and  $b(|\mathbf{x}|) = O(|\mathbf{x}| - 1)$  as  $|\mathbf{x}| \searrow 1$ , so that

1. The  $m_{\rho,\varepsilon_k}(\mathbf{x})$  are smooth functions in  $B_L$ ;
2. The  $m_{\rho,\varepsilon_k}(\mathbf{x})$  approximate  $M_1$  as  $\varepsilon_k \rightarrow 0$  and then  $\rho \rightarrow 0$ . Namely, the operators  $-\nabla \cdot m_{r,\varepsilon}^{-1} \nabla$  converge (as described below) to  $-\nabla \cdot M_1^{-1} \nabla$  as  $\varepsilon_k \rightarrow 0$  and  $\rho \rightarrow 0$ . Note that these  $a(|\mathbf{x}|), b(|\mathbf{x}|)$  are independent of  $\rho$ .

Below we use the shorthand notation  $\varepsilon \rightarrow 0$  instead of  $\varepsilon_k \rightarrow 0$ . Denote

$$\begin{aligned} \tilde{\theta}(\mathbf{x}) &= a(|\mathbf{x}|) \int_0^1 p_1(r') dr' + b(|\mathbf{x}|) \int_0^1 p_2(r') dr' + \int_0^1 p_3(r') dr', \quad 1 < |\mathbf{x}| < 2, \\ \tilde{\theta}(\mathbf{x}) &= 1, \quad |\mathbf{x}| < 1 \text{ or } |\mathbf{x}| > 2. \end{aligned} \quad (35)$$

We can choose  $p_i(r'), i = 1, 2$  to be smooth functions that are very close to the characteristic functions of the intervals  $(0, 1/2)$  and  $(1/2, 1)$ , continued periodically, while  $p_3(r')$  has its support very close to  $r' = 0$ , continued periodically. To have that the Hamiltonians corresponding to  $m_{\rho,\varepsilon}$  to approximate Hamiltonian corresponding to  $M_1$  (cf. [23] for analysis of the  $\Gamma$ -convergence and the two-scale convergence of these operators) we need that

$$\frac{1}{2}(a(r) + b(r)) \approx 2, \quad \frac{1}{2} \left( \frac{1}{a(r)} + \frac{1}{b(r)} \right) \approx \frac{1}{2(r-1)},$$

i.e.,

$$a(r) \approx 2(1 + \sqrt{2-r}), \quad b(r) \approx 2(1 - \sqrt{2-r}), \quad 1 < r < 2. \quad (36)$$

Thus, the mass density  $m_{\rho,\varepsilon}(|\mathbf{x}|)$  corresponds to two materials occupying layers of equal width in each cell with those cells separated by a very thin layer of uniform density.

Making a Liouville gauge transformation for equation (17), that is, introducing

$$\psi_{\rho,\varepsilon}(\mathbf{x}) = m_{\rho,\varepsilon}^{-1/2}(\mathbf{x}) u_{R,\varepsilon}(\mathbf{x}), \quad (37)$$

(33) becomes the Schrödinger equation with potential  $V_{\rho,\varepsilon}$ ,  $\text{supp}(V_{\rho,\varepsilon}) \subset \overline{B_2} - B_1$ . Here,  $\text{supp}(V_{\rho,\varepsilon})$ , the *support* of  $V_{\rho,\varepsilon}$ , is the set where  $V_{\rho,\varepsilon}(\mathbf{x})$  is non-zero. For generic values of the parameters, these model approximate invisibility cloaks for matter waves [22], with Schrödinger equations

$$(-\nabla \cdot \nabla + V_{\rho,\varepsilon} + Q_\rho - E)\psi_{\rho,\varepsilon} = 0 \quad \text{in } B_L, \quad u|_{\partial B_L} = h. \quad (38)$$

Here  $E = \omega^2$ , and these *cloaking potentials*,  $V_{\rho,\varepsilon}$ , are of the form,

$$\begin{aligned} V_{\rho,\varepsilon}(\mathbf{x}) - E &= m_{R,\varepsilon}^{1/2} \nabla \cdot \nabla (m_{R,\varepsilon}^{-1/2}) - E m_{R,\varepsilon} \kappa_R, \quad R < |\mathbf{x}| < 2, \\ V_{\rho,\varepsilon}(\mathbf{x}) &= 0, \quad 0 < |\mathbf{x}| < R \text{ and } 2 < |\mathbf{x}| < 3. \end{aligned} \quad (39)$$

In addition, inside the cloak, i.e. in  $B_1$ , there is the *cloaked potential* (cf. (10))

$$Q_\rho(\mathbf{x}) = -E(\eta(\mathbf{x}; \tau) - 1), \quad \text{supp}(Q_\rho) \subset \overline{B_{R_0}} \subset B_1, \quad (40)$$

where  $\tau = \tau^{\text{sen}}(R, \omega)$  and  $Q_\rho$  depends on the parameter  $\tau(R, \omega)$ . Thus, when  $\tau$  is appropriately chosen, the total potential  $V_{\rho,\varepsilon} + Q_\rho$  in  $B_L$  acts as a quantum mechanical sensor cloak. It is this *total* potential which we call a *Schrödinger hat* (SH). (The cloaked potential, that is,  $Q_\rho$ , resembles a “hat”, specifically the Mexican hat, but the terminology is chosen because of the interesting effects of the potential, not because of its profile.)

### Analysis of Schrödinger’s hat: convergence of normalization constants

To consider the properties of a Schrödinger’s hat, one first needs some convergence properties of approximate cloaks as they approach an ideal one, initially treating the case when  $E$  is not a Dirichlet eigenvalue of Laplacian in the ball of radius  $L$ . The case of Dirichlet eigenvalues will be considered later.

Let  $u$  satisfy the boundary value problem

$$\begin{aligned} (-\nabla \cdot \nabla - E)u &= 0, \quad \text{in } B_L \subset \mathbb{R}^3, \\ u|_{\partial B_L} &= h. \end{aligned} \quad (41)$$

Moreover, let

$$Q_0 = \lim_{\rho \rightarrow 0} Q_\rho = E(1 - \eta(\mathbf{x}; (\tau_1(R_0, \tau_2), \tau_2))),$$

(see (40)), be the potentials supported in  $B_{R_0}$ , with the parameters suppressed. Then the  $Q_0$  describe QM cloaked sensor potentials at energy  $E$ .

Let  $F = F_R$  with  $R = 1$  be the singular blow up map and define

$$\tilde{u}(\mathbf{x}) = \begin{cases} u(F^{-1}(\mathbf{x})), & \text{for } \mathbf{x} \in B_L - \overline{B}_1, \\ \beta u(0)\Phi(\mathbf{x}), & \text{for } \mathbf{x} \in \overline{B}_1, \end{cases} \quad (42)$$

where  $\beta = \Phi(1)^{-1}$  and  $u$  is the solution of (41).

Let  $u_\rho$  be a solution of Helmholtz equation

$$\begin{aligned} (-\nabla \cdot M_R^{-1} \nabla + Q_\rho - E\kappa_R)u_\rho &= 0, \quad \text{in } B_L \subset \mathbb{R}^3, \\ u_\rho|_{\partial B_L} &= h, \end{aligned} \quad (43)$$

and  $u_{\rho,\varepsilon}$  be a solution of Helmholtz equation,

$$\begin{aligned} (-\nabla \cdot m_{\rho,\varepsilon}^{-1} \nabla + Q_\rho - E\kappa_R)u_{\rho,\varepsilon} &= 0, \quad \text{in } B_L \subset \mathbb{R}^3, \\ u_{\rho,\varepsilon}|_{\partial B_L} &= h. \end{aligned} \quad (44)$$

Then,

$$\lim_{\varepsilon \rightarrow 0} u_{\rho,\varepsilon} = u_\rho, \quad (45)$$

in the space  $L^2(B_L)$ . Moreover, letting  $K \subset B_L - B_1$  be arbitrary, using (35), (37), one can show that

$$\lim_{\rho \rightarrow 0} \lim_{\varepsilon \rightarrow 0} \int_K |\psi_{\rho,\varepsilon}(\mathbf{x})|^2 d\mathbf{x} = \lim_{\rho \rightarrow 0} \lim_{\varepsilon \rightarrow 0} \int_K m_{\rho,\varepsilon}(\mathbf{x})^{-1} |u_{\rho,\varepsilon}(\mathbf{x})|^2 d\mathbf{x} = \int_K \tilde{\theta}(\mathbf{x}) |\tilde{u}(\mathbf{x})|^2 d\mathbf{x}. \quad (46)$$

Proofs of the claims (45) and (46) are omitted and will be detailed elsewhere, but the principal ideas are that, using the above properties of the spherical harmonics expansions,

$$\lim_{\rho \rightarrow 0} \lim_{\varepsilon \rightarrow 0} u_{\rho,\varepsilon}(\mathbf{x}) = \tilde{u}(\mathbf{x}) \quad \text{for } \mathbf{x} \in B_L - \partial B_1, \quad (47)$$

and that, for  $\phi \in C(\overline{B}_L)$ ,

$$\lim_{\rho \rightarrow 0} \lim_{\varepsilon \rightarrow 0} \int_K m_{\rho,\varepsilon}^{-1}(\mathbf{x}) \phi(\mathbf{x}) d\mathbf{x} = \int_K \tilde{\theta}(\mathbf{x}) \phi(\mathbf{x}) d\mathbf{x}. \quad (48)$$

In the following, we use

$$\psi^{eff}(\mathbf{x}) = \tilde{\theta}(\mathbf{x})^{1/2} \tilde{u}(\mathbf{x}) \quad (49)$$

which can be considered as the effective wave function, when one is modeling the location of the particle corresponding to the wave function  $u_{\rho,\varepsilon}$  with sufficiently small  $\rho$  and  $\varepsilon$ .

### Conditional probabilities for location of particles in a Schrödinger hat

Consider next the situation of two balls of radius  $L$ , one empty and the other with a Schrödinger hat potential, and assume that there is one particle in each ball. Let  $u(\mathbf{x})$  be wave function corresponding to the particle in the empty ball and  $\psi_{\rho,\varepsilon}$  be the wave function corresponding to the ball with the SH potential. Assume that  $u$  and  $\psi_{\rho,\varepsilon}$  have the same boundary value,  $h$ , on  $\partial B_L$ .

Consider next the normalization constants

$$\begin{aligned} C_3^{empty} &= \int_{B_L - B_2} |u(\mathbf{x})|^2 d\mathbf{x}, \\ C_2^{empty} &= \int_{B_2 - \bar{B}_1} |u(\mathbf{x})|^2 d\mathbf{x}, \\ C_1^{empty} &= \int_{B_1} |u(\mathbf{x})|^2 d\mathbf{x}, \\ C_3^{cloak} &= \lim_{\rho \rightarrow 0} \lim_{\varepsilon \rightarrow 0} \int_{B_L - B_2} |\psi_{\rho,\varepsilon}(\mathbf{x})|^2 d\mathbf{x}, \\ C_2^{cloak} &= \lim_{\rho \rightarrow 0} \lim_{\varepsilon \rightarrow 0} \int_{B_2 - \bar{B}_1} |\psi_{\rho,\varepsilon}(\mathbf{x})|^2 d\mathbf{x}, \\ C_1^{cloak} &= \lim_{\rho \rightarrow 0} \lim_{\varepsilon \rightarrow 0} \int_{B_1} |\psi_{\rho,\varepsilon}(\mathbf{x})|^2 d\mathbf{x}. \end{aligned}$$

The probability that a free particle  $X$  in the empty ball  $B_L$ , described by the wave function  $u$ , is in fact located in the smaller ball  $B_1$ , is equal to

$$\mathbb{P}(\{X \in B_1\}) = \frac{C_1^{empty}}{C_1^{empty} + C_2^{empty} + C_3^{empty}}.$$

Similarly, the probability that a particle  $\tilde{X}_{\rho,\varepsilon}$  in the ball  $B_L$  with the SH potential  $V_{\rho,\varepsilon} + Q_\rho$ , described by the wave function  $\psi_{\rho,\varepsilon}$ , to be in  $B_1$  satisfies

$$\lim_{\rho \rightarrow 0} \lim_{\varepsilon \rightarrow 0} \mathbb{P}(\{\tilde{X}_{\rho,\varepsilon} \in B_1\}) = \frac{C_1^{cloak}}{C_1^{cloak} + C_2^{cloak} + C_3^{cloak}}.$$

Similar results hold for the probabilities for the particles to be in  $B_2 - B_1$  and  $B_L \setminus B_2$ .

Using (46)–(48), we see that

$$\begin{aligned} C_3^{cloak} &= C_3^{empty}, \\ C_1^{cloak} &= \frac{1}{|\Phi(1)|^2} |u(0)|^2. \end{aligned}$$

Recall that  $u$  is the solution of (41) and  $\Phi$  is the  $L^2(B_1)$ -normalized Neumann eigenfunction inside the cloak, cf. (42). As for  $C_2^{cloak}$ , by (46) and (49), we have

$$C_2^{cloak} = \int_{B_2 \setminus B_1} |\psi^{eff}(\mathbf{x})|^2 d\mathbf{x} = \int_{B_2 \setminus B_1} \tilde{\theta}(\mathbf{x}) |\tilde{u}(\mathbf{x})|^2 d\mathbf{x} = \int_{B_2} \theta(\mathbf{y}) |u(\mathbf{y})|^2 d\mathbf{y}, \quad (50)$$

$$\theta(\mathbf{y}) = \tilde{\theta}(\mathbf{x}) \left| \frac{\partial \mathbf{x}}{\partial \mathbf{y}} \right|, \quad \mathbf{x} = F(\mathbf{y}), \quad |\mathbf{y}| < 2.$$

From the definition of  $F(\mathbf{y})$ , cf. (5), one sees that  $\theta(\mathbf{y}) = O\left(\frac{1}{|\mathbf{y}|^2}\right)$ ; however, due to the boundedness of the norm of  $u$  in the space  $H^1(B_L)$ , the integral in (50) is bounded. An important observation is that, by changing the parameters  $\tau$  determining the potentials  $Q_\rho$ ,  $Q_0$ , *one can keep  $C_3^{\text{cloak}}$  and  $C_2^{\text{cloak}}$  unchanged while  $C_1^{\text{cloak}}$  is made arbitrarily large.*

Consider a particle  $X$  with energy  $E$  in an empty ball  $B_L$  and another particle  $\tilde{X}_{\rho,\varepsilon}$  with energy  $E$  in the same box but with the SH potential  $V_{\rho,\varepsilon} + Q_\rho$ . Let us next consider the event that the particle  $X$  in the empty ball corresponding to wave function  $u$  is located in the set  $S \subset B_L$ , and denote this event by  $L_S$ . Then,

$$\mathbb{P}(L_S) = c_{\text{empty}} \int_S |u(\mathbf{x})|^2 d\mathbf{x}, \quad c_{\text{empty}} = \frac{1}{C_1^{\text{empty}} + C_2^{\text{empty}} + C_3^{\text{empty}}}.$$

The conditional probability for the event that the particle  $X$  is in  $S \subset B_L \setminus B_2$ , conditioned on the particle being in  $S_0 := B_L \setminus B_2$ , is thus

$$\mathbb{P}(L_S | L_{S_0}) = \frac{\int_S |u(\mathbf{x})|^2 d\mathbf{x}}{\int_{S_0} |u(\mathbf{x})|^2 d\mathbf{x}}. \quad (51)$$

Next, for a ball  $B_L$  in which there is an SH potential, denote the event that a particle  $\tilde{X}_{\rho,\varepsilon}$  is located in the set  $S \subset B_L \setminus B_2$  by  $\tilde{L}_S(\rho, \varepsilon)$ . Then,

$$\begin{aligned} \mathbb{P}(\tilde{L}_S(\rho, \varepsilon)) &= c_{\text{cloak}}(\rho, \varepsilon) \int_S |\psi_{\rho,\varepsilon}(\mathbf{x})|^2 d\mathbf{x}, \\ \lim_{\rho \rightarrow 0} \lim_{\varepsilon \rightarrow 0} c_{\text{cloak}}(\rho, \varepsilon) &= \frac{1}{C_1^{\text{cloak}} + C_2^{\text{cloak}} + C_3^{\text{cloak}}}. \end{aligned}$$

Thus, the conditional probability for the event that the particle  $X$  is in  $S \subset B_L \setminus B_2$ , conditioned on it being in  $S_0 := B_L \setminus B_2$ , is

$$\mathbb{P}(\tilde{L}_S(\rho, \varepsilon) | \tilde{L}_{S_0}(\rho, \varepsilon)) = \frac{\int_S |\psi_{\rho,\varepsilon}(\mathbf{x})|^2 d\mathbf{x}}{\int_{S_0} |\psi_{\rho,\varepsilon}(\mathbf{x})|^2 d\mathbf{x}}, \quad (52)$$

and

$$\lim_{\rho \rightarrow 0} \lim_{\varepsilon \rightarrow 0} \mathbb{P}(\tilde{L}_S(\rho, \varepsilon) | \tilde{L}_{S_0}(\rho, \varepsilon)) = \mathbb{P}(L_S | L_{S_0}). \quad (53)$$

In summary, the above computations have the following consequences for the wave functions  $u$  and  $\psi_{\rho,\varepsilon}$ , corresponding to the particles in an empty ball and a ball with the SH potential, resp. Recall that the both field  $u$  and  $\psi_{\rho,\varepsilon}$  have the boundary value  $h$ . Then, under the condition that we

observe a particle in  $B_L \setminus B_2$ , the conditional probability that the particle is observed to be in a set  $S \subset B_L \setminus B_2$ , conditioned on it being observed to be in a set  $B_L \setminus B_2$ , is same for both balls.

Consider now the case when  $S = B_1$ , or, more generally,  $S \subset B_{R_0} \subset B_1$ . Clearly, equations (51)–(52) remain valid for such  $S$ . However, equation (53) is no longer valid. Moreover, by choosing properly parameters  $\tau$ , we can make  $\lim_{\rho \rightarrow 0} \lim_{\varepsilon \rightarrow 0} \mathbb{P}(\tilde{L}_S(\rho, \varepsilon) | \tilde{L}_{S_0}(\rho, \varepsilon))$  as large as we want. To measure this effect we introduce the ratio

$$\mathfrak{S} = \lim_{\rho \rightarrow 0} \lim_{\varepsilon \rightarrow 0} \frac{1}{|u(0)|^2} \int_{B_1} |\psi_{\rho, \varepsilon}(\mathbf{x})|^2 d\mathbf{x} = \frac{1}{|\Phi(1)|^2}, \quad (54)$$

see (42), (49), where  $\tilde{\theta}(\mathbf{x}) = 1$  in  $B_1$ ; we call  $\mathfrak{S}$  the *strength* of the SH potential  $Q_0$ .  $\mathfrak{S}$  depends only on the choice of the parameters  $\tau(\rho, \omega) = (\tau_1, \tau_2)$ , in particular, the parameter  $\tau_2$  that determines how rapidly the solution grows in the layer  $B_{s_2} \setminus B_{s_1} \subset B_{R_0}$ . Choosing  $\tau(\rho, \omega)$  appropriately, we can achieve any prescribed positive value of  $\mathfrak{S}$ . The parameters  $(\tau_1, \tau_2)$  of the SH potential do not change the (non-normalized) wave function outside the ball  $B_1$  but change radically the wave in it. The wave inside the ball  $B_1$  has the variance of momentum  $\mathfrak{S}|u(0)|^2 \int_{B_1} |\nabla \Phi(\mathbf{x})|^2 d\mathbf{x}$  and the charge  $Q'$  considered later in formula (69). We consider the function inside  $B_1$  as a quasi-particle and introduce a solid state model for in Section .

We analyzed above the eigenfunction in a ball, and it was enough to analyze only the lowest harmonic. One can replace the ball  $B_L$  with an arbitrary domain  $\Omega \subset \mathbb{R}^3$  containing the ball  $B_L$  where the cloaked SH potential is supported using the following observation: The boundary value problem

$$\begin{aligned} (-\nabla \cdot \nabla + V_{\rho, \varepsilon} + Q_\rho - E)\psi_{\rho, \varepsilon} &= 0 = 0 \quad \text{in the domain } \Omega, \\ \psi_{\rho, \varepsilon} &= h \quad \text{on the boundary } \partial\Omega, \end{aligned} \quad (55)$$

is equivalent to the problem

$$\begin{aligned} (-\nabla \cdot \nabla - E)\psi_{\rho, \varepsilon} &= 0 \quad \text{in the domain } \Omega - B_L, \\ \psi_{\rho, \varepsilon} &= h \quad \text{on the boundary } \partial\Omega, \\ \nu \cdot \nabla \psi_{\rho, \varepsilon}|_{\partial B_L} &= \Lambda_{\rho, \varepsilon}(\psi_{\rho, \varepsilon}|_{\partial B_L}) \quad \text{on the boundary } \partial B_L, \end{aligned} \quad (56)$$

where  $\Lambda_{\rho, \varepsilon}$  is the Dirichlet-to-Neumann operator for the equation  $(-\nabla \cdot \nabla + V_{\rho, \varepsilon} + Q_\rho - E)\psi = 0$  in the ball  $B_L$ . The previous analysis for the higher order harmonics shows that the Dirichlet-to-Neumann operators  $\Lambda_{\rho, \varepsilon}$  for the ball with the SH potential tend, as  $\rho$  and  $\varepsilon$  tend to zero, to

the Dirichlet-to-Neumann operator corresponding to an empty ball. Thus, the above analysis of the behavior of the solutions in the ball  $B_L$  can be readily generalized to an arbitrary domain  $\Omega$ . Potentials which, for *some* incident wave, produce a scattered wave which is zero outside a bounded set, are said to have a *transmission eigenvalue* [35]. We emphasize that the scattered wave caused by the SH potential is approximately zero for *all* incident fields.

An illustrative example of this phenomenon via quantum three-card monte is described in the body of the paper.

### Scattering from the hat and particle storage

Now consider the effect of Schrödingers hats on scattering experiments in  $\mathbb{R}^3$ . In the case of free space, the wave function  $\Psi$  satisfies

$$(-\nabla \cdot \nabla - E)\Psi = 0, \quad \text{in } \mathbb{R}^3, \quad (57)$$

and we can choose

$$\Psi(\mathbf{x}) = \Psi^{in}(\mathbf{x}) = e^{i\omega(\mathbf{e}, \mathbf{x})}, \quad |\mathbf{e}| = 1, \quad \omega^2 = E,$$

so that  $\Psi^{in}(\mathbf{x})$  are the plane waves in the direction  $\mathbf{e}$ . Compare them with the wave functions in  $\mathbb{R}^3$  corresponding to scattering from the SH potential,

$$\begin{aligned} (-\nabla \cdot \nabla + V_{\rho, \varepsilon} + Q_\rho - E)\Psi_{\rho, \varepsilon} &= 0, \quad \text{in } \mathbb{R}^3, \\ \Psi_{\rho, \varepsilon} &= \Psi^{in} + \Psi_{\rho, \varepsilon}^{sc}, \end{aligned} \quad (58)$$

where  $\Psi_{\rho, \varepsilon}^{sc}(\mathbf{x})$  satisfies Sommerfeld's radiation condition. Note that the SH potential  $V_{\rho, \varepsilon} + Q_\rho$  vanishes outside  $B_2$ .

As scattering data for these problems is equivalent to Dirichlet-to-Neumann operators on  $\partial B_L$  [36], we can use previous results to consider scattering from the SH potential. In particular, we see using (37), (42), and (45), that when  $\rho$  and  $\varepsilon$  are small enough, the solution  $\Psi_{\rho, \varepsilon}(\mathbf{x})$  is close to  $\Psi^{in}(\mathbf{x})$  outside  $B_2$ , close to  $m_{\rho, \varepsilon}^{-1/2}(\mathbf{x})\Psi^{in}(F^{-1}(\mathbf{x}))$  in  $B_2 - B_R$ , and close to  $\Psi^{in}(0)\Phi(\mathbf{x})$  in the cloaked region.

Thus, we see that scattering observations, i.e., observables depending on the far field patterns of the solutions, are almost the same for the empty space and for the Schrödinger hat potential

(when  $\rho$  and  $\varepsilon$  are small enough). However, if we consider the conditional probability of particles in an empty ball and one with the SH potential, i.e., the ratios

$$I_{S_1, S_2} = \frac{\int_{S_1} |\psi(\mathbf{x})|^2 d\mathbf{x}}{\int_{S_2} |\psi(\mathbf{x})|^2 d\mathbf{x}}$$

and

$$\tilde{I}_{S_1, S_2} = \frac{\int_{S_1} |\psi_{\rho, \varepsilon}(\mathbf{x})|^2 d\mathbf{x}}{\int_{S_2} |\psi_{\rho, \varepsilon}(\mathbf{x})|^2 d\mathbf{x}}.$$

we see that one can make  $\tilde{I}_{S_1, S_2} \gg I_{S_1, S_2}$  if  $S_1$  contains  $B_1$  and  $S_2$  does not intersect  $B_2$ . The physical interpretation of this is that, when a particle scatters from a Schrödinger hat, there is a high concentration of probability mass in the cloaked region, but this can not be detected from far field observations.

#### A hat and two ions - an interaction amplifier

A SH potential also amplifies the interaction between two charged particles. To see this, consider two particles of the same species, which for simplicity we simply refer to as *ions*. Suppose that one ion, having energy  $E$ , is confined to a domain which also includes a SH potential  $V_{SH}$ , centered at point  $O$ . Tuning the parameters of the SH potential, the probability that the ion is concentrated in a ball  $B_d$ , of small radius  $d$  and center  $O$ , can be made as close to 1 as desired. If one now inserts *two* ions into the domain which interact both with the potential  $V_{SH}$  and with each other via a Coulomb potential, both charged particles can not be concentrated in  $B_d$ . First-order perturbation theory shows [?] that the energy level of the particles in the presence of a SH behaves as if the charges of the ions were multiplied by a (large) factor  $O(d^{-1/2})$ .

Let us consider a large ball  $B_L$  (we could also consider a box  $D_L = [-L, L]^3$  or any other domain) containing a SH potential and a single particle system modeled by

$$(-\nabla \cdot \nabla + V_{\rho, \varepsilon}(\mathbf{x}) + Q_{\rho}(\mathbf{x}) - E)\psi_{\rho, \varepsilon}(\mathbf{x}) = 0 \text{ in } B_L, \quad \psi_{\rho, \varepsilon}|_{\partial B_L} = 0, \quad \|\psi_{\rho, \varepsilon}\|_{L^2(B_L)} = 1, \quad (59)$$

cf. (38). Here  $E > 0$  is the Dirichlet eigenvalue of the partial differential operator in (41) in the empty ball  $B_L$ , corresponding to radially symmetric eigenfunction  $\psi^0(\mathbf{x}) = j_0(\omega|\mathbf{x}|)$ ,  $\omega = \sqrt{E}$ , so that  $j_0(\omega L) = 0$ , and  $V_{\rho, \varepsilon}(\mathbf{x})$ ,  $Q_{\rho}(\mathbf{x})$  are chosen as in the subsection. I.C. In addition to the



one-particle equation, we consider a system of two charged particles, modeled by

$$\begin{aligned} (-\nabla_x \cdot \nabla_x - \nabla_y \cdot \nabla_y + V_{\rho,\varepsilon}(\mathbf{x}) + Q_\rho(\mathbf{x}) + V_{\rho,\varepsilon}(\mathbf{y}) + Q_\rho(\mathbf{y}) + \frac{a}{|\mathbf{x} - \mathbf{y}|} - 2E')\Psi(\mathbf{x}, \mathbf{y}) &= 0, \\ \text{in } (\mathbf{x}, \mathbf{y}) \in B_L \times B_L, \\ \Psi|_{\partial(B_L \times B_L)} &= 0, \end{aligned} \quad (60)$$

where the energy  $2E'$  is close to  $2E$ . Here,  $a$  is proportional to the product of charges of the ions. When  $a$  is small (which we now assume), the solution  $\Psi$  is a perturbation of  $\Psi^0$ , the product of two one-particle solutions,

$$\Psi^0(\mathbf{x}, \mathbf{y}) = \psi_{\rho,\varepsilon}(\mathbf{x})\psi_{\rho,\varepsilon}(\mathbf{y}). \quad (61)$$

By first-order perturbation theory, we can write

$$\begin{aligned} E' &= E + aE_1 + O(a^2), \\ \Psi(\mathbf{x}, \mathbf{y}) &= \Psi_{\rho,\varepsilon}^{(0)}(\mathbf{x}, \mathbf{y}) + a\Psi_{\rho,\varepsilon}^{(1)}(\mathbf{x}, \mathbf{y}) + O(a^2), \quad \Psi_{\rho,\varepsilon}^{(1)}|_{\partial(B_L \times B_L)} = 0. \end{aligned} \quad (62)$$

We will show that the two-particle interaction is strongly effected by the presence of a SH.

Substituting approximation (62) in equation (60) and considering terms of order  $O(a)$ , we obtain the equation

$$\begin{aligned} &(-\nabla_x \cdot \nabla_x - \nabla_y \cdot \nabla_y + V_{\rho,\varepsilon}(\mathbf{x}) + Q_\rho(\mathbf{x}) + V_{\rho,\varepsilon}(\mathbf{y}) + Q_\rho(\mathbf{y}) - 2E)\Psi_{\rho,\varepsilon}^{(1)}(\mathbf{x}, \mathbf{y}) \\ &= \left(2E_1 - \frac{1}{|\mathbf{x} - \mathbf{y}|}\right) \Psi_{\rho,\varepsilon}^{(0)}(\mathbf{x}, \mathbf{y}), \quad \text{for } (\mathbf{x}, \mathbf{y}) \in B_L \times B_L, \quad \Psi_{\rho,\varepsilon}^{(1)}|_{\partial(B_L \times B_L)} = 0 \end{aligned} \quad (63)$$

As  $2E$  is the eigenvalue of the left hand side of (63) with  $\Psi_{\rho,\varepsilon}^{(0)}$  being its eigenfunction, it is necessary that

$$E_1 = \frac{1}{2} \int_{B_L} \int_{B_L} \frac{1}{|\mathbf{x} - \mathbf{y}|} |\psi_{\rho,\varepsilon}(\mathbf{x})|^2 |\psi_{\rho,\varepsilon}(\mathbf{y})|^2 d\mathbf{x} d\mathbf{y}, \quad (64)$$

where we have used (61), (59). Let

$$\Phi_L(\mathbf{x}) = \int_{B_L} \Psi_{\rho,\varepsilon}(\mathbf{x}, \mathbf{y}) \overline{\psi_{\rho,\varepsilon}(\mathbf{y})} d\mathbf{y}, \quad \Phi_L^{(1)}(\mathbf{x}) = \int_{B_L} \Psi_{\rho,\varepsilon}^{(1)}(\mathbf{x}, \mathbf{y}) \overline{\psi_{\rho,\varepsilon}(\mathbf{y})} d\mathbf{y}.$$

Multiplying (63) by  $\overline{\psi_{\rho,\varepsilon}(\mathbf{y})}$ , integrating over  $B_L$  in  $\mathbf{y}$ , and using integration by parts yields

$$\begin{aligned} &(-\nabla_x \cdot \nabla_x + V_{\rho,\varepsilon}(\mathbf{x}) + Q_\rho(\mathbf{x}) - E) \Phi_L^{(1)}(\mathbf{x}) \\ &= 2E_1 \psi_{\rho,\varepsilon}(\mathbf{x}) - V_{eff}(\mathbf{x}) \psi_{\rho,\varepsilon}(\mathbf{x}), \end{aligned} \quad (65)$$

with the effective potential given by

$$V_{eff}(\mathbf{x}) = \int_{B_L} \frac{1}{|\mathbf{x} - \mathbf{y}|} |\psi_{\rho,\varepsilon}(\mathbf{y})|^2 d\mathbf{y}. \quad (66)$$

Next, we compare the above results with the case when a single particle scatters from the potential which is the sum of to the SH potential  $V_{\rho,\varepsilon}(\mathbf{x}) + Q_\rho(\mathbf{x})$  and the potential  $V_{eff}(\mathbf{x})$  multiplied by parameter  $a$ , that is the equation

$$(-\nabla \cdot \nabla + V_{\rho,\varepsilon}(\mathbf{x}) + Q_\rho(\mathbf{x}) + aV_{eff}(\mathbf{x}) - E^{eff}) \phi^{eff}(\mathbf{x}) = 0 \text{ in } B_L, \quad \phi^{eff}|_{\partial B_L} = 0. \quad (67)$$

First-order perturbation theory then implies that

$$\begin{aligned} E^{eff} &= E + 2aE_1 + O(a^2) = E' + O(a^2), \\ \phi^{eff}(\mathbf{x}) &= \psi_{\rho,\varepsilon}(\mathbf{x}) + a\Phi_L^{(1)}(\mathbf{x}) + O(a^2) = \Phi_L(\mathbf{x}) + O(a^2). \end{aligned}$$

Thus, when two particles are in a ball containing a SH potential, each particle behaves, up to error  $O(a^2)$ , as if the other particle and the SH potential were replaced by the potential  $V_{\rho,\varepsilon}(\mathbf{x}) + Q_\rho(\mathbf{x}) + aV_{eff}$ .

To analyze  $V_{eff}$ , let  $\mathfrak{S}$  be the strength of the SH potential, as defined in (54). Note that by choosing  $\tau$  appropriately, we can make  $\mathfrak{S}$  arbitrarily large and, for such  $\mathfrak{S}$ , the  $L^2$  normalized waves are strongly concentrated in  $B_R$ . For large  $\mathfrak{S}$  and every  $\mathbf{x} \in B_L$ ,

$$\int_{B_L \setminus B_R} \frac{1}{|\mathbf{x} - \mathbf{y}|} |\psi_{\rho,\varepsilon}(\mathbf{y})|^2 d\mathbf{y} << \int_{B_R} \frac{1}{|\mathbf{x} - \mathbf{y}|} |\psi_{\rho,\varepsilon}(\mathbf{y})|^2 d\mathbf{y}. \quad (68)$$

Recall that the potential  $Q_\rho$  is constructed so that the solution inside the cloak is concentrated in a ball  $B_{R_0}$ , and assume next that  $R_0 > 0$  is small. To emphasize this, we denote  $R_0 = \delta << 1$ . One then obtains

$$V_{eff}(\mathbf{x}) \approx \int_{B_1} \frac{1}{|\mathbf{x} - \mathbf{y}'|} |\psi_{\rho,\varepsilon}(\mathbf{y}')|^2 dy' \approx \frac{Q'}{|\mathbf{x}|}, \quad Q' = \int_{B_1} |\psi_{\rho,\varepsilon}(\mathbf{y}')|^2 dy' \quad (69)$$

Thus,  $\Phi_L(\mathbf{x})$  satisfies a one-particle Schrödinger equation where the potential is a SH potential slightly modified by a Coulomb one with charge  $aQ'$  at the origin.

Compare this with the case when we have no SH potential but add the Coulomb interaction. Analyze this using first-order perturbation theory, writing the wave function and the energy as

$$\begin{aligned} \Phi^{Cou}(\mathbf{x}) &= \phi^{empty}(\mathbf{x}) + a\phi_1^{Cou}(\mathbf{x}) + O(a^2), \\ E^{Cou} &= E + aE_1^{Cou} + O(a^2), \end{aligned}$$

where  $\phi^{empty}(\mathbf{x}) = c_L j_0(\omega_0|x|)$  and  $c_L > 0$  is such that  $\|\phi^{empty}\|_{L^2(B_L)} = 1$ . Analogously to (65), one obtains

$$\begin{aligned} -\nabla \cdot \nabla \phi_1^{Cou}(\mathbf{x}) - E^{Cou} \phi_1^{Cou}(\mathbf{x}) + a\mathcal{V}(\mathbf{x})\phi_1^{Cou}(\mathbf{x}) &= O(a^2), \quad \text{in } B_L \setminus 0, \\ \phi_1^{Cou}|_{\partial B_L} &= 0, \end{aligned} \quad (70)$$

where

$$\mathcal{V}(\mathbf{x}) = \int_{B_L} \frac{1}{|\mathbf{x} - \mathbf{y}'|} |\phi^{empty}(\mathbf{y}')|^2 dy'$$

and

$$E_1^{Cou} = \frac{1}{2} \int_{B_L} \int_{B_L} \frac{1}{|\mathbf{x} - \mathbf{y}|} |\phi^{empty}(\mathbf{x})|^2 |\phi^{empty}(\mathbf{y})|^2 d\mathbf{x} d\mathbf{y}. \quad (71)$$

Now compare  $E_1$  defined for the Coulomb and SH potentials with the analogous quantity  $E_1^{Cou}$  defined for the Coulomb potential (with no SH potential). Consider the case when  $\mathfrak{S}$  and  $c_L$  are of the same size, and when the potential  $Q_\rho$  is constructed so that the solution inside the cloak is concentrated in a ball  $B_\delta$ , where  $\delta > 0$  is small. Then formula (64) implies that we have  $E_1 = O(\delta^{-1})$ . When  $\delta$  is very small, the value  $aE_1$ , i.e., the change in the energy level, is much larger than in the Coulomb case without SH potential. Thus, by engineering the potential  $Q_\rho$  appropriately, one can make the SH cloak increase the interaction caused by the Coulomb potential: When two particles are put in a ball with a SH potential, the energy level of the particles is changed as if the charges of the particles were multiplied by a factor of  $O(\delta^{-1/2})$ . The energy level coefficient  $E_1$  then approaches infinity as  $\delta \rightarrow 0$ , and thus for small  $\delta$  one has that  $E_1 \gg E_1^{Cou}$ . This means that the presence of the SH potential has strengthened the Coulomb interaction of the particles, effectively increasing repulsion between the particles.

## NUMERICAL SIMULATIONS

**Simulation of eigenfunctions and comparison with free space.** The results above may be illustrated using numerical simulations. For Fig. 3 we compute the effective field  $\psi^{eff}$  for the Dirichlet eigenfunctions in ball  $B_L$  where in the ball have in  $B_2$  the SH potential we use  $\rho = 0.01$ ,  $L = 2\pi$ ,  $E = 4$  and inside the cloak we have a potential  $Q_0$  represented in the form

$$Q_0(r) = \tau_1 \chi_{r < s_1} + \tau_2 \chi_{s_1 < r < s_2}. \quad (72)$$

using parameters  $s_1 = 0.6$ ,  $s_2 = 0.8$ ,  $\tau_2 = -50$ . Using Matlab, we found the value  $\tau_1 = 12.9016$  corresponding to the SH potential. In the figures we will visualize the effective field

$$\psi^{eff}(\mathbf{x}) = \begin{cases} \tilde{\theta}(\mathbf{x})^{\frac{1}{2}} u(F^{-1}(\mathbf{x})), & \text{for } \mathbf{x} \in B_L \setminus \overline{B_1}, \\ \beta u(0) \Phi(\mathbf{x}), & \text{for } \mathbf{x} \in \overline{B_1}, \end{cases} \quad (73)$$

defined in formulas (42) and (49), see also the formula (46).

Let  $R_a = 3$  and  $A_{empty}$  be the event “the particle in the empty ball is in the layer  $\{R_a < |x| < L\}$ ” and  $A_{SH}$  be the event “the particle in the ball with the SH potential is in the layer  $\{R_a < |x| < L\}$ ”. Then

$$\mathbb{P}(A_{empty}) = 0.5021, \quad \mathbb{P}(A_{SH}) = 0.1355.$$

Additionally, let  $B_{empty}$  be the event “the particle in the empty ball is in the layer  $\{2 < |x| < L\}$ ” and  $B_{SH}$  the event “the particle in the ball with the SH potential is in the layer  $\{2 < |x| < L\}$ ”, i.e., the particle is outside the cloaking device. We obtain

$$\mathbb{P}(B_{empty}) = 0.7196, \quad \mathbb{P}(B_{SH}) = 0.1941.$$

The conditional probabilities that the particle is in  $\{R_a < |x| < L\}$ , conditioned on it being in the layer  $\{2 < |x| < R_L\}$ , are given by

$$\mathbb{P}(A_{empty}|B_{empty}) = \mathbb{P}(A_{SH}|B_{SH}) = 0.6977.$$

This shows that when the SH potential is inserted in the ball  $B_L$ , the particle is observed in the region  $B_2 - B_1$  with a lower probability but, when it is observed, the observations from it are similar to the observations one would have if the ball were empty.

**Numerical simulation of the scattered wave.** We compute scattering solutions for the SH potential using spherical harmonics  $n \leq N = 70$  and  $|m| \leq n$ . In Fig. 1 we plot the total field corresponding to the plane wave with energy  $E = 256$  which scatters from the SH potential supported in the ball  $B_2$ . The figure shows the real part of the effective field in the ball  $B_L$ ,  $L = 3$  in the plane  $z = 0$ . The SH potential corresponds to the parameter  $\rho = 0.01$  and the potential  $Q_0$  is represented in the form (72) with  $s_1 = 0.25$ ,  $s_2 = 0.5$ ,  $\tau_2 = -10$ . Using Matlab, we found the value  $\tau_1 = -169.49$  corresponding to the SH potential.

**Simulation of different modes of the cloak.** We next visualize the above choice of parameters using numerical simulations of the scattering problem. We compute the real part of effective field

corresponding to the total field when we have an incoming plane wave, where in the ball  $B_2$  there is a potential consisting of a cloaking potential  $V_{\rho,\varepsilon}$  plus a potential  $Q_0$  supported in the cloaked region. We use energy  $E = 4$ , and for the cloaking potential we use the parameter  $\rho = 0.01$  and the potential  $Q_0$  is given in the form (72) with parameters  $s_1 = 0.6$ ,  $s_2 = 0.8$ ,  $\tau_2 = -25$ . Using Matlab, we found the value  $\tau_1 = 7.0675$  corresponding to SH potential. We computed the corresponding effective field,  $\psi_{SH}^{eff}$ , defined in formula (73). To show different modes of the cloak, we perturbed the parameter  $\tau_1$  to the value  $\tau_1^{cloak} = 8.2531$  corresponding to the cloak mode and computed the corresponding effective field  $\psi_{cloak}^{eff}$ . In addition, we perturbed the parameter  $\tau_1$  to the value  $\tau_1^{res} = 7.120$  corresponding to the resonance mode and computed the corresponding effective field  $\psi_{res}^{eff}$ . All fields are computed using spherical harmonics  $n \leq N = 30$  and  $|m| \leq n$ , and the real parts of the fields are plotted in Fig. 2 on the positive  $x$ -axis  $\{(x, 0, 0) : x \in [0, 3]\}$ .

## IMPLEMENTATION OF THE SH POTENTIALS

Equation (33) with isotropic mass  $m_{\rho,\varepsilon}$  and bulk modulus  $\kappa_R$  describes an approximate acoustic cloak. The negative values of  $\tau_2$  required in our construction of potential  $Q_\rho$  corresponds then to a material with a negative bulk modulus; such materials have already been proposed [37]. There are many proposals for acoustic cloaks [6–8, 20]; implementing an acoustic cloak and placing negative bulk modulus material inside the cloak, one could test the concept of the SH potential in the acoustic setting.

For electromagnetic waves, one can consider a cylindrical electromagnetic cloak [5] and insert in it material with negative permittivity to implement a structure similar to the SH potential. The analysis related to such cylindrical cloaks with suitable chosen parameters to create a SH potential for incident TM-polarized waves is similar to the analysis for the 3D cloak considered in this paper (with different asymptotics of coefficients (30)).

Next we consider approximate quantum cloaks and Schrödinger hat potentials.

To implement an anisotropic Schrödinger hat, one could consider a quantum cloak with an anisotropic effective mass and include the potential  $Q_\rho$  in the cloaked region. Possible realizations of quantum cloaks have been proposed by Zhang et al. [9], using crystal structures in an optical lattice at ultra-low temperatures, which make possible a large variation of the effective mass. Below, using the Liouville gauge transformation (37), we propose a realization of the SH potential using solid state models which do not require large variation of the effective mass.

The function  $V_{\rho,\varepsilon}$  is a rapidly oscillating radially symmetric potential, and we can use the homogenization theory to approximate the SH potential  $V_{\rho,\varepsilon} + Q_\rho$  by a piecewise constant radially symmetric function,

$$V_{SH}(\mathbf{r}) = \sum_{j=1}^N V_j \chi_j^{(1)}(|\mathbf{r}|), \quad \mathbf{r} \in \mathbb{R}^3,$$

where  $\chi_j^{(1)}$  are indicator functions of suitably chosen intervals  $I_j^{(1)} = [a(j), b(j)]$  and  $V_j$  are constants. Applying homogenization theory one can see that the solutions corresponding to  $V_{SH}$  with sufficiently large  $N$  approximate the solutions corresponding to  $V_{\rho,\varepsilon} + Q_\rho$  when  $V_j$  are chosen appropriately. In fact, it is enough to use potentials for which the constants  $V_j$  have only two different values, one very negative and one very positive. Thus, we can form an approximate SH potential using layers of spherical potential wells of depth  $-V_-$  and barrier walls of height  $V_+$ , i.e.,

$$V_{SH}(\mathbf{r}) = \sum_{j=1}^{N_1} V_+ \chi_j^+(|\mathbf{r}|) - \sum_{j=1}^{N_2} V_- \chi_j^- (|\mathbf{r}|)$$

where  $\chi_j^\pm$  are indicator functions of the suitably chosen intervals  $I_j^\pm = [a^\pm(j), b^\pm(j)]$ . Note that the two-scale homogenization theory used for the above approximation does not specify how large  $N$  one needs to use, but just states that the convergence to the correct limit happens as  $N$  grows.

Let us choose the physical units so that  $m_0 = 1$  is the effective mass of the particle which we consider and that  $\hbar = 2^{1/2}$ . If  $\psi$  satisfies

$$\left(-\frac{\hbar^2}{2m_0} \nabla \cdot \nabla + V_{SH}(\mathbf{r}) - E\right) \psi(\mathbf{r}) = 0,$$

then by scaling the length variable by  $\ell$ , we see that  $\Psi(\mathbf{r}) = \psi(\mathbf{r}/\ell)$  satisfies

$$\left(-\frac{\hbar^2}{2m_0} \nabla \cdot \nabla + \ell^{-2} V_{SH}(\mathbf{r}/\ell) - \ell^{-2} E\right) \Psi(\mathbf{r}) = 0. \quad (74)$$

When  $\ell$  is very large, this means that the energy level  $E$  is replaced by a new, much smaller energy level  $\ell^{-2}E$  and the depth of the potential wells are replaced by much shallower wells, and the height of the barrier walls are replaced by much lower walls. We denote  $V_{SH,\ell}(\mathbf{r}) = \ell^{-2}V_{SH}(\mathbf{r}/\ell)$  and  $E_\ell = \ell^{-2}E$ . When the above potential  $V_{\rho,\varepsilon} + Q_\rho$  is defined using energy  $E$  in formulas (39) and (40), we say that  $V_{SH,\ell}$  is designed to operate at the energy level  $E_\ell$ .

To consider models appearing in solid state physics, we have to consider an effective mass depending on the  $x$  variable. So, now consider four materials with isotropic (i.e., spherical) effective masses  $m_1, m_2, m_3, m_4$ , such that  $m_1 \leq m_2 \leq m_3 \leq m_4$  and  $m_1 \leq m_0 \leq m_4$  and potentials

$V_1, V_2, V_3, V_4$  corresponding to the conduction band edge energies. Assume that the maximum of  $V_j$  is larger than the maximum  $V_{SH,\ell}$  and the minimum of  $V_j$  is smaller than the minimum  $V_{SH,\ell}$ . We next study spherical layers of these materials, with abrupt interfaces between materials.

Let us consider a structure consisting of many thin spherical layers of these four materials which near  $|\mathbf{r}| = r$  are mixed according to ratios  $\ell_1(r), \ell_2(r), \ell_3(r), \ell_4(r) \in [0, 1]$ , correspondingly. We need these ratios to satisfy the system

$$\ell_1(r) + \ell_2(r) + \ell_3(r) + \ell_4(r) = 1, \quad (75)$$

$$m_1\ell_1(r) + m_2\ell_2(r) + m_3\ell_3(r) + m_4\ell_4(r) = m_0,$$

$$\frac{\ell_1(r)}{m_1} + \frac{\ell_2(r)}{m_2} + \frac{\ell_3(r)}{m_3} + \frac{\ell_4(r)}{m_4} = \frac{1}{m_0},$$

$$V_1\ell_1(r) + V_2\ell_2(r) + V_3\ell_3(r) + V_4\ell_4(r) = V_{SH,\ell}(\mathbf{r}).$$

Below, we assume that  $m_j, V_j, E_\ell$ , and  $\ell^{-2}V_\pm$  are such that the solution of the system (75) satisfies  $\ell_1(r), \ell_2(r), \ell_3(r), \ell_4(r) \in [0, 1]$ . By means of homogenization theory, one can see that when the equations (75) hold, we can approximate the SH potential using a configuration where spherical layers of materials  $(m_j, V_j)$  are combined at the energy level  $E_\ell$ , as is shown below. Note that if the masses  $m_j$  are equal to  $m_0$  we need only two materials and approximate the SH potential with spherical quantum wells of given depth  $-\ell^{-2}V_-$  and walls of height  $\ell^{-2}V_+$ . In the general case when the masses are different, we need four different materials to solve equations (75).

Now consider the situation where we have spherical layers

$$L_j = B_{R(j)} - B_{R(j-1)} \subset \mathbb{R}^3, \quad j = 1, 2, \dots, 4J$$

with  $0 \leq R(j) < R(j+1) \leq 2$ . Let  $\psi$  be the wave function corresponding to the particle in this layered structure. Then in the each layer we have Schrödineger equation

$$\left(-\frac{\hbar^2}{2}\nabla \cdot \frac{1}{m_i}\nabla + V_i - E_\ell\right)\psi(\mathbf{r}) = 0, \quad x \in L_j, \quad i = i(j) \quad (76)$$

and  $i(j) \in \{1, 2, 3, 4\}$  indicates which material is present in the layer  $L_j$ . We may choose  $i(j) \equiv j \bmod 4$  and

$$R(j+1) - R(j) = \frac{1}{2J}\ell_{i(j)}(R(j)).$$

On the interfaces of the layers, that is, at  $r = R(j)$ , we impose the BenDaniel-Duke boundary conditions [42]

$$\psi|_{r=R(j)+} = \psi|_{r=R(j)-}, \quad \frac{1}{m_{i(j+1)}}\partial_r\psi|_{r=R(j)+} = \frac{1}{m_{i(j)}}\partial_r\psi|_{r=R(j)-}. \quad (77)$$

Similar Hamiltonians and the appropriate boundary conditions in various heterostructures are discussed extensively in the reference [38]. When number of layers  $4J \gg N$ , the solutions of the obtained equations approximate the solutions of the equation (74), on related mathematical theory, cf. [23, 39].

We now propose how the above model could be physically implemented using effective-mass theory to approximate electrons in semiconductors. Consider a semiconductor heterostructure build up using four semiconductor materials having the same lattice structures, such as  $\text{Al}_x\text{Ga}_{1-x}\text{As}$  with mixing parameter  $x$  having the values  $x_1, x_2, x_3$ , and  $x_4$  where  $0 \leq x_j \leq 1$ , and assume that the lowest energies in each conduction band (the conduction band edge) in these materials corresponds to the wave vector  $\mathbf{k}_0 = 0$ . Using Bastard's envelope function approximation [29, 40], we consider in the heterostructure the wave function  $\psi(\mathbf{r})$ , corresponding to the energy  $\mathcal{E}$  being close to a conduction band edge, which in each material can be expanded as

$$\psi(\mathbf{r}) = \sum_n f_n(\mathbf{r}) u_n(\mathbf{r}, \mathbf{k}_0) \quad (78)$$

where the sum in  $n$  is taken over the finite number of energy bands. Here,  $f_n(\mathbf{r})$  are the slowly varying envelope functions and  $u_n(\mathbf{r}, \mathbf{k}_0)$  are the periodic Bloch functions in the material corresponding to wave vector  $\mathbf{k}_0$ . We also assume that the Bloch functions are the same in all four materials. Next we consider the single band analysis of electrons near the lowest conduction band energy and study the wave function  $\psi(\mathbf{r})$  omitting in the sum (78) all other values of  $n$  except the value  $n_0$  corresponding to the lowest energy in the conduction band. This means that we use the approximation

$$\psi(\mathbf{r}) = f_{n_0}(\mathbf{r}) u_{n_0}(\mathbf{r}, \mathbf{k}_0). \quad (79)$$

For the GaAs-Ga(Al)As heterostructures, with sufficiently thick GaAs layers, the above approximation (79), with the Schrödinger equations

$$\left(-\frac{\hbar^2}{2} \nabla \cdot \frac{1}{m_i} \nabla + V_i - \mathcal{E}\right) f_{n_0}(\mathbf{r}) = 0, \quad \mathbf{r} \in L_j, \quad i = i(j), \quad (80)$$

and the BenDaniel-Duke interface conditions (77) for the single band envelope function  $f_{n_0}(\mathbf{r})$ , have been proposed in [29, Sec. 3.II.2.3] and [41]. Similar models have also been proposed for other 3D heterostructures in [38, 42].

Now suppose that the spherically layered semiconductor structure described above is located in the ball  $B_2$ ; surround it with a similar heterostructure having effective mass  $m_0$  and the conduction



band edge energy  $V_0$ , being normalized to have the value  $V_0 = 0$ . We note that above we could have assumed that, e.g.,  $m_2 = m_0$  and  $V_2 = 0$  in which case the surrounding material may be homogeneous semiconductor material. To consider the scattering of electrons traveling in the medium having the energy  $\mathcal{E}$ , one can study the Dirichlet-to-Neumann operator  $\Lambda : h \mapsto \partial_\nu f_{n_0}|_{\partial B_2}$  for the boundary value problem,

$$\begin{aligned} \left(-\frac{\hbar^2}{2}\nabla \cdot \frac{1}{m(\mathbf{r})}\nabla + V(\mathbf{r})\right)f_{n_0}(\mathbf{r}) &= \mathcal{E}f_{n_0}(\mathbf{r}), \quad \text{for } \mathbf{r} \in B_2, \\ f_{n_0}(\mathbf{r})|_{\partial B_2} &= h, \end{aligned} \quad (81)$$

see (55)-(56). Here,  $m(\mathbf{r}) = m_{i(j)}$  and  $V(\mathbf{r}) = V_{i(j)}$  in spherical layers  $L_j \subset B_2$ .

As the number of layers,  $J$ , grows, the envelope function  $f_{n_0}(\mathbf{r})$  approaches [23, 39] the solution of the Schrödinger equation  $(-\frac{\hbar^2}{2m_0}\nabla \cdot \nabla + V_{SH,\ell} - \mathcal{E})f = 0$  and, moreover, the Dirichlet-to-Neumann map  $\Lambda$  of the equation (81) approaches the Dirichlet-to-Neumann operator corresponding to the equation

$$-\frac{\hbar^2}{2}\nabla \cdot \frac{1}{m_0}\nabla f^{hom}(\mathbf{r}) = \mathcal{E}f^{hom}(\mathbf{r}), \quad \text{for } \mathbf{r} \in B_2$$

corresponding to the homogeneous background. Thus, the scattering of electrons caused by the heterostructure in  $B_2$  is very small but the wave function may be very large inside the ball  $B_1$ . We emphasize that  $V_{SH}$  depends on the energy level  $E_\ell$ , see (39) and (40), and thus the above analysis applies only for electrons whose energy  $\mathcal{E}$  is close to  $E_\ell$ .

We note that the above theoretical model can be considered as a (much) more complicated structure than the spherical semiconductor layer construction previously used to implement quantum dots [43] and a related construction of cylindrical semiconductor layers [44].

Let us also discuss the distribution of the energies of electrons in the heterostructure with conduction band edge energy  $\mathcal{E}_c$ . The density function of the energies of the electrons in the conduction band is the product

$$n(\mathcal{E}) = D(\mathcal{E})f(\mathcal{E})$$

of the density of states  $D(\mathcal{E})$  and the Fermi-Dirac distribution  $f(\mathcal{E}) = C(e^{(\mathcal{E}-\mu)/(k_B T)} + 1)^{-1}$ , where  $T$  is the temperature,  $\mu < \mathcal{E}_c$  is the Fermi energy,  $k_B$  is Boltzmann's constant, cf. [45, Sec. 1.4] and [46, Sec. 8], and  $C$  is the normalization constant. The density of states  $D(\mathcal{E})$  is usually approximated by  $C(\mathcal{E}-\mathcal{E}_c)^{1/2}$ ,  $\mathcal{E} > \mathcal{E}_c$  near  $\mathcal{E}_c$ . When the Fermi-Dirac distribution is approximated by Maxwell-Boltzmann distribution  $f_{mb}(\mathcal{E}) = Ce^{-(\mathcal{E}-\mu)/(k_B T)}$ , one sees that the density of the

energy  $\mathcal{E} - \mathcal{E}_c$  is approximately distributed according to the Gamma distribution with the shape parameter  $3/2$  and the scale parameter  $k_B T$ . Then the energies have the expectation

$$\mathcal{E}_{av} = \mathcal{E}_c + \frac{3}{2}k_B T$$

and the variance  $\frac{3}{2}(k_B T)^2$ . Thus, the energies near the conduction band edge  $\mathcal{E}_c$  are crucial in the modeling of semiconductors, and at low temperatures  $T$  the density of electrons,  $n(\mathcal{E})$ , is concentrated near the average  $\mathcal{E}_{av}$ .

By the above, when the temperature  $T$  is low enough, then the energies of the electrons in the conduction band have a distribution concentrated near the energy level  $\mathcal{E}_{av}$ . Thus by perturbing a homogeneous semiconductor material by including in it one or several SH potentials  $V_{SH,\ell}$ , designed to operate at the energy level  $E_\ell = \mathcal{E}_{av}$ , one can create a device where most of the electrons would behave in the above analysis: The non-normalized wave functions of electrons would not be perturbed outside the supports of the SH potentials but the amplitude of the wave functions are strongly amplified inside the support of the SH potentials.

In summary: Assume that we have layers of semiconducting materials where the electrons with energy near the edge of the conduction band can be modeled by a Schrödinger equation (81) and that in these semiconducting materials the effective masses and the potentials have slightly different values. Then, appropriate choices of layer thickness and a sufficiently large heterostructure lead to the envelope functions of the wave functions satisfying the Schrödinger equation for a SH potential.

**Acknowledgments:** AG is supported by US NSF; YK by UK EPSRC; ML by Academy of Finland; and GU by US NSF, a Walker Family Endowed Professorship at UW, a Chancellor Professorship at UC, Berkeley, and a Clay Senior Award.

- 
- [1] A. Greenleaf, M. Lassas, G. Uhlmann, *Physiol. Meas.* **24**, 413 (2003).
  - [2] A. Greenleaf, M. Lassas, G. Uhlmann, *Math. Res. Lett.* **10**, 685 (2003).
  - [3] U. Leonhardt, *Science* **312**, 1777 (2006).
  - [4] J. Pendry, D. Schurig, D. Smith, *Science* **312**, 1780 (2006).
  - [5] D. Schurig, *et al.*, *Science* **314**, 977 (2006).
  - [6] S. Cummer, D. Schurig, *New J. Phys.* **9**, 45 (2007).
  - [7] H.Y. Chen, C.T. Chan, *Appl. Phys. Lett.* **91**, 183518 (2007)

- [8] S. Cummer, *et al.*, *Phys. Rev. Lett.* **100**, 024301 (2008).
- [9] S. Zhang, D. Genov, C. Sun, X. Zhang, *Phys. Rev. Lett.* **100**, 123002 (2008).
- [10] H.Y. Chen, C.T. Chan, *Appl. Phys. Lett.* **90**, 241105 (2007).
- [11] A. Greenleaf, Y. Kurylev, M. Lassas, G. Uhlmann, *Phys. Rev. Lett.* **99**, 183901 (2007).
- [12] Y. Lai, *et al.*, *Phys. Rev. Lett.* **102**, 253902 (2009).
- [13] A. Greenleaf, Y. Kurylev, M. Lassas, G. Uhlmann, *Phys. Rev. E* **83**, 016603 (2011).
- [14] R. Parr, W. Yang, *Density-Functional Theory of Atoms and Molecules* (Oxford UP, 1994).
- [15] R. Shelby, D. Smith, S. Schultz, *Science* **292**, 77 (2001).
- [16] J. Li, C.T. Chan, *Phys. Rev. E* **70**, 055602(R) (2004).
- [17] S.H. Lee, *et al.*, *Phys. Rev. Lett.* **104**, 054301 (2010).
- [18] H.Y. Chen, C.T. Chan, *J. Phys. D: Appl. Phys.* **43**, 113001 (2010).
- [19] [http://en.wikipedia.org/wiki/Quantum\\_paradox](http://en.wikipedia.org/wiki/Quantum_paradox)
- [20] A. Greenleaf, Y. Kurylev, M. Lassas, G. Uhlmann, *Comm. Math. Phys.* **275**, 749 (2007).
- [21] A. Greenleaf, Y. Kurylev, M. Lassas, G. Uhlmann, <http://arxiv.org/abs/0801.3279> (2008).
- [22] A. Greenleaf, Y. Kurylev, M. Lassas, G. Uhlmann, *Phys. Rev. Lett.* **101**, 220404 (2008).
- [23] A. Greenleaf, Y. Kurylev, M. Lassas, G. Uhlmann, *J. Spectral Theory* **1**, 27 (2011).
- [24] A. Alù, N. Engheta, *Phys. Rev. Lett.* **102**, 233901 (2009).
- [25] J. Zuloaga, E. Prodan, P. Nordlander, *Nano Lett.* **9**, 887 (2009).
- [26] J. Fransson, H. Manoharan, A. Balatsky, *Nano Lett.* **10**, 1600 (2010).
- [27] F. Zolla, S. Guenneau, A. Nicolet, J. Pendry, *Opt. Lett.* **32**, 1069 (2007).
- [28] A. Alù, N. Engheta, *Phys. Rev. Lett.* **105**, 263906 (2010).
- [29] G. Bastard, *Wave Mechanics Applied to Semiconductor Heterostructures* (Halsted Pr., 1988).
- [30] Z. Ruan, M. Yan, C. Neff, M. Qiu, *Phys. Rev. Lett.* **99**, 113903 (2007).
- [31] A. Greenleaf, Y. Kurylev, M. Lassas, G. Uhlmann, *New J. Phys.* **10**, 115024 (2008).
- [32] R. Kohn, H. Shen, M. Vogelius and M. Weinstein, *Inv. Prob.* **24**, 015016 (2008).
- [33] R. Kohn, D. Onofrei, M. Vogelius, M. Weinstein, *Comm. Pure Appl. Math.* **63**, 1525 (2010).
- [34] M. Abramowitz, I. Stegun, *Handbook of Mathematical Functions with Formulas, Graphs, and Mathematical Tables* (Dover, 1972).
- [35] D. Colton, L. Päiväranta, J. Sylvester, *Inv. Prob. Imag.* **1**, 13 (2006).
- [36] Y. Berezanskii, *Trudy Moskov. Mat. Obsch.* **7**, 1 (1958).
- [37] Y. C. Wang, R. S. Lakes, *Journal of Composite Materials* **39**, 1645 (2005).

- [38] R. Morrow, *Phys. Rev. B* **36**, 4836 (1987).
- [39] G. Allaire, A. Piatnitski, *Comm. Math. Phys.* **258**, 1-22 (2005).
- [40] G. Bastard, *Phys. Rev. B* **24**, 5693-5697 (1981)
- [41] G. Bastard, J. Brum, *IEEE J. Quantum Elect.* **9**, 1625 - 1644 (1986)
- [42] J. BenDaniel, C. Duke, *Phys. Rev.* **152**, 683-692 (1966)
- [43] D. Schooss, A. Mews, A. Eychmüller, H. Weller, *Phys. Rev. B* **49**, 17072 (1994)
- [44] N. V. Tkach, I. V. Pronishin, A. M. Makhnety, *Phys. Solid State* **40**, 514 (1998).
- [45] S. Sze, *Physics of Semiconductor Devices*. Wiley-Interscience, (2nd Ed.), 1981, 880 pp
- [46] C. Kittel, *Introduction to Solid State Physics* (7th Ed.), Wiley, (1996).